Hydrogeology Journal (2022) 30:511–532
https://doi.org/10.1007/s10040-021-02446-5

PAPER

Hydrochemical-geophysical study of saline paleo-water contamination in alluvial aquifers

Giorgio Pilla[1] · **Patrizio Torrese**[1]

Received: 26 June 2021 / Accepted: 26 December 2021 / Published online: 26 January 2022

Abstract

An integrated hydrochemical and geophysical study of the saline paleo-water uprising into the alluvial aquifer of the Oltrepò Pavese plain sector (Po Plain, northern Italy) is presented. This study involved hydrochemical analysis of groundwater, assessment of well logs, and one-, two- and three-dimensional electrical geophysical surveys. The studied area was selected for its characteristic hydrogeological setting. The alluvial aquifer is strongly conditioned by the presence of a buried tectonic discontinuity along which the saline waters are mainly distributed. These waters rise along the discontinuities in the bedrock and flow into the overlying alluvial aquifer. Contamination from saline waters is not spatially and vertically homogeneous within the aquifer. The spatial distribution of Na–Cl waters suggests the existence of plumes of highly mineralized waters that locally reach the aquifer, diffuse and mix with freshwaters. The saline waters show a dilution during upward migration, which is due to mixing with the shallow fresh groundwater. Highly mineralized groundwater is identified even at very shallow depth in correspondence with each plume. On the other hand, there is a lower degree of contamination in those sectors of the aquifer that are further away from the structural discontinuities and this lesser contamination generally only involves the deeper parts of the aquifer.

Keywords Hydrochemistry · Geophysical study · Saline water · Contamination · Alluvial aquifers

Introduction

Saline paleo-water uprising into aquifers is a hydrogeological process controlled by the geological and structural setting of the area, and the mechanisms are often not fully understood (Barberio et al. 2021; Conti et al. 2000; Grobe and Machel 2002; Petitta et al. 2011; Re and Zuppi 2011; Schwartz and Muehlenbachs 1979; Yechieli and Sivan 2010). While down-flowing fluids may be of meteoric origin, uprising fluids may connect the lowermost parts of an aquifer with the surface. An aquifer's contamination by saline water is caused by mixing of freshwaters with brines—examples can be found in the European countries Belgium, Denmark, England (UK), Estonia, France, Italy and Spain (Darling et al. 1997; Desiderio and Rusi 2004; Dever et al. 2001; Hinsby et al. 2001; Bonnesen et al. 2009; Marandi and Vallner 2010; Petitta et al. 2011), and in Kansas and Texas in the USA (Stueber et al. 1998). Aquifer contamination can also be found where the fossil salt water, located far from the coastline, is the remainder of ancient marine ingressions, for example in Togo, Morocco and Vietnam (Akouvi et al. 2008; Bouchaou et al. 2009). Saline groundwater may result in environmental problems and difficulties in the exploitation and management of the aquifer, not only for drinking-water supply, but also for agricultural and industrial use. Contamination with salty water may not be spatially and vertically homogeneous within the aquifer. Intrusion and mixing of salt water with fresh groundwater of the shallow aquifer may result in different degrees of groundwater salinity within the aquifer.

Typically, an unfavorable distribution of sampling wells makes it necessary to integrate any hydrogeological and hydrochemical study with geophysical surveys (Di Sipio et al. 2006; Fadili et al. 2017; Jiraporn et al. 2020; Kouzana et al. 2010; Pilla et al. 2010; Pujari et al. 2012; Torrese and Pilla 2021). This allows definition of the general hydrogeological setting of the studied area, as well as detailed characterization of localized and restricted zones of the aquifer where the uprising phenomenon of deep saline waters

✉ Patrizio Torrese
patrizio.torrese@unipv.it

[1] Dipartimento di Scienze della Terra e dell'Ambiente, Università di Pavia, Pavia, Italy

occurs. This integrated and multidisciplinary approach is crucial for the understanding of this particular form of natural contamination which is often strictly controlled by the peculiar geological and structural configuration of the area and which can be influenced by several intervening factors.

This paper presents an integrated hydrochemical and geophysical study of the saline paleo-water uprising into the alluvial aquifer of the Oltrepò Pavese plain sector (Po Plain, northern Italy). Here, the alluvial aquifer is strongly conditioned by the presence of the Vogherese Fault, a buried tectonic discontinuity along which the saline waters are mainly distributed (Pilla et al. 2007), which is responsible for the uprising of deep, saline paleo-waters. This contamination prevents the exploitation of the aquifer, not only for drinking-water supply (Italian Legislative Decree, Decreto Legislativo 2 febbraio 2001, n. 31, Italian Legislature 2001), but also for agricultural (Wilcox 1948) and industrial uses.

The presence of these saline waters is known in the investigated area, as well as throughout the Po Plain area at the bottom of the Apennine mountain range front, the areas of the Po Plain that correspond to bedrock structural reliefs (Bonori et al. 2000; Toscani et al. 2007; Di Sipio et al. 2007), and the Central Apennine foredeep (Nanni and Zuppi 1986; Desiderio and Rusi 2004). Even so, their distribution and the mechanisms that control their uprising into the shallow aquifer (like withdrawals and changes of total head) are little understood. Torrese and Pilla (2021) investigated a test site of the Oltrepò Pavese plain sector; they found that the bedrock is affected by saline-water contamination in localized areas that are likely associated with structural discontinuities, which facilitate the flow towards the alluvial aquifer. They also found localized and restricted zones of salinization within the aquifer (Cameron et al. 2018).

The aims of this study are the chemical and geophysical characterization of the aquifer, definition of the extent of saline-water contamination, estimation of the depth to the freshwater/salt-water interface, monitoring of the variation in salinity over time, and the carrying out of a detailed and accurate investigation of localized zones of salinization within the aquifer.

The integration of hydrochemical and geophysical investigations aims to obtain further insights into the spatial distribution of saline-water contamination and the mechanisms underlying the upward migration of saline paleo-water, its intrusion and mixing with the fresh groundwater of the shallow aquifer.

This study included periodical sampling of groundwater to monitor the chemistry and temperature, vertical electrical conductivity and temperature logs to monitor the salt-water/freshwater transition zone, and geophysical surveys. These involved both electromagnetic (EM) surveys over vast areas for a speedy assessment of subvertical conductive bodies connected to the uprising of high-salinity waters through structural discontinuities, and accurate one-dimensional (1D) to 3D electrical resistivity surveys for detailed investigation of the sectors where the uprising phenomena of deep saline waters occurs.

Chemical–physical characterization of groundwater

In case of high hydrochemical variability of groundwater, a hydrochemical survey (groundwater sampling from wells and chemical analysis) is typically used to distinguish different types of waters and their origin and evolution (Appelo and Postma 2005).

In coastal aquifers affected by seawater ingressions, in addition to conventional hydrochemical investigations, multiparameter well logs play a key role in the identification and characterization of the ingress of salt waters in the aquifers.

The systematic use of probes equipped with sensors for temperature (Polemio et al. 2009; Vandenbohede et al. 2014) and electrical conductivity measurements (Cotecchia et al. 1999; Smart and Worthington 2003; Di Sipio et al. 2006; Polemio et al. 2009; Tal et al. 2019; Shin and Hwang 2020) allows for the collection of significant and rapid data, albeit qualitative, on the chemical-physical characteristics of the groundwater.

During the data acquisition phase, particular attention must be paid to the descent velocity of the multiparameter probes along the water column of the wells. The descent velocity must be sufficiently low (<0.03 m/s) as to not disrupt the chemical stratification of the groundwaters (Cotecchia et al. 1999).

The Oltrepò Pavese plain sector is affected by saline-water uprising into the alluvial aquifer. This is a hydrogeological process that has common aspects with seawater ingression. For this reason, well logs were expected to be particularly useful in the Oltrepò Pavese plain sector to identify the vertical distribution of saline water into the aquifer. Moreover, the repetition of the measurements in the most significant wells during different periods of the year was expected to allow characterization of the variation over time in the distribution of saline water.

VLF-EM and electric resistivity methods

Electromagnetic and electrical resistivity methods are geophysical techniques well suited to the investigation and (partial) characterization of aquifers. The theory that underlies the very-low-frequency electromagnetic (VLF-EM) technique is well described in the literature (Paterson and Ronka 1971; Phillips and Richards 1975; Ramesh Babu et al. 2007). The VLF-EM technique is a passive method that uses radiation from worldwide ground-based military radio transmitters used

for navigation operating in the VLF band (15–30 kHz) as the primary EM field.

VLF-EM has been typically used to prospect for conductive mineral deposits (Paal 1965) and for the identification of fracture zones for groundwater exploration (Jamal and Singh 2018), detection of fractures in the bedrock (Adepelumi et al. 2006), geological boundaries and shear zones/faults (Gnaneshwar et al. 2011; Parker 1980; Phillips and Richards 1975; Saydam 1981, Ramesh Babu et al. 2007; Sundararajan et al. 2006), but it has been also applied to map groundwater conditions in sedimentary basins (Ohwoghere-Asuma et al. 2020) and to detect leachate plumes and groundwater pollution (Al-Tarazi et al. 2008).

Electrical resistivity methods allow characterization of subsurface materials in terms of their electrical properties. They involve the application of direct current into the ground by means of two current electrodes and measurement of the resulting voltage via two potential electrodes. The arrangement of current and potential electrodes during the measurement is dependent on the chosen electrode array. Each array provides different vertical and lateral resolution and depth of penetration (Kneisel 2006; Schrott and Sass 2008; Smith 1986; Szalai and Szarka 2008; Szalai et al. 2009). To obtain a true resistivity model of the subsurface, an inversion procedure is needed (Loke and Barker 1996). The three main methods of electrical resistivity surveys are resistivity depth sounding (RDS), resistivity profiling (RP), and electric imaging, commonly termed electrical resistivity tomography (ERT). ERT provides an image of the subsurface electrical resistivity pattern and allows for identification of subsurface structures. Its theory (Arato et al. 2014; Athanasiou et al. 2007; Buvat et al. 2013; Dahlin and Loke 1998; Daily and Owen 1991; Loke et al. 2003; Spiegel et al. 1980) and application (Cassiani et al. 2009; Daily and Ramirez 1992; Griffiths and Barker 1993; Guérin and Benderitter 1995; Guérin et al. 2004; Kuras et al. 2009; Ritz et al. 1999; Torrese 2020) are well-documented in geophysical literature.

There have been many applications of ERT and electrical methods in general to characterize aquifers (Coscia et al. 2011; Meyerhoff et al. 2014; Vogelgesang et al. 2020), to delineate alluvial aquifer heterogeneity (Bowling et al. 2005), thickness and bedrock structure (Gómez et al. 2019), to monitor hydraulic processes (Kuras et al. 2009) and aquifer discharge (Meyerhoff et al. 2012), to map saline-water contamination (Kazakis et al. 2016; Rainone et al. 2015), and to detect karst features (Torrese 2020), sinkholes and cavities (Torrese et al. 2021; Van Schoor 2002).

Hydrogeological setting

The Oltrepò Pavese plain sector is geologically characterized by alluvial Quaternary deposits that cover Miocene–Pliocene marine deposits with very low hydraulic conductivity, formed by soils with a high clay content (clays, sandy clays, sandy-marls, sandstones, conglomerates, gypsum-rich marls and calcareous marls (Pellegrini and Vercesi 1995)).

The upper Quaternary deposits, deposited mainly by the action of the Po River and by the Apennine streams, represent the main water-bearing units of the area. Three different hydrogeological units can be defined within the Quaternary deposits: pre-Würmian alluvial deposits, middle-ancient alluvial deposits, and recent and present alluvial deposits (Cavanna et al. 1998; Pilla et al. 2007; Fig. 1). Only the latter two hydrogeological units are affected by the presence of sodium chloride (Na–Cl) rich waters.

The middle-ancient alluvial deposits occupy most of the Oltrepò Pavese plain sector and are formed by alternating sands and gravels, with interbedded clays or clayey silts. The recent and present alluvial deposits, distributed mainly along the Po River, were originated by the post-Würmian depositional activity of this river. The most important Apennine streams also contributed to the deposition of these alluvial deposits. Moreover, the continuous presence of a clayey silty covering, which has a varying maximum thickness of 10–15 m, in the sectors close to the Apennine margin, and a minimum of 2 m in the meandering area of the Po River, limits infiltration and influences the aquifer recharge that occurs in correspondence of the coalescent fans originating from the deposition of Apennine streams (Pilla et al. 2007). A recharge contribution from the Po River must be excluded. In fact, groundwater flow direction (Fig. 2) is towards the River Po with the exception of occasional flooding events (Pilla et al. 2007). The aquifer is a single-bedded unconfined aquifer, although it becomes locally and temporarily (during some periods of the year) confined due to the presence of the clayey silty covering.

The structural setting of the Oltrepò Pavese plain is strongly conditioned by the presence of an important tectonic discontinuity, known in literature as the Vogherese Fault (Boni 1967) (Fig. 1). This fault, which is buried below a few tens of meters of alluvial deposits, has a NE–SW direction at a regional scale, from west of Casteggio to the Colle of S. Colombano (in the area of Pavia plain), passing across the confluence of the Ticino and Po rivers (Boni 1967). It is suggested that it is a normal fault with hanging wall to the NE, up to the Barbianello area. Here, it becomes an inverse fault to the south of Pinarolo, folding gradually towards the west, north of Casteggio and Voghera. Given the absence of specific recent studies on the subject, and since the definition of the fault type is outside the scope of this study, the Vogherese Fault has always been traced as a vertical fault on the cross-sections of this paper. The Vogherese Fault is responsible for the sudden deepening that affects the hydrogeological bedrock in the northern sector of the Oltrepò Pavese plain, and is also responsible for the

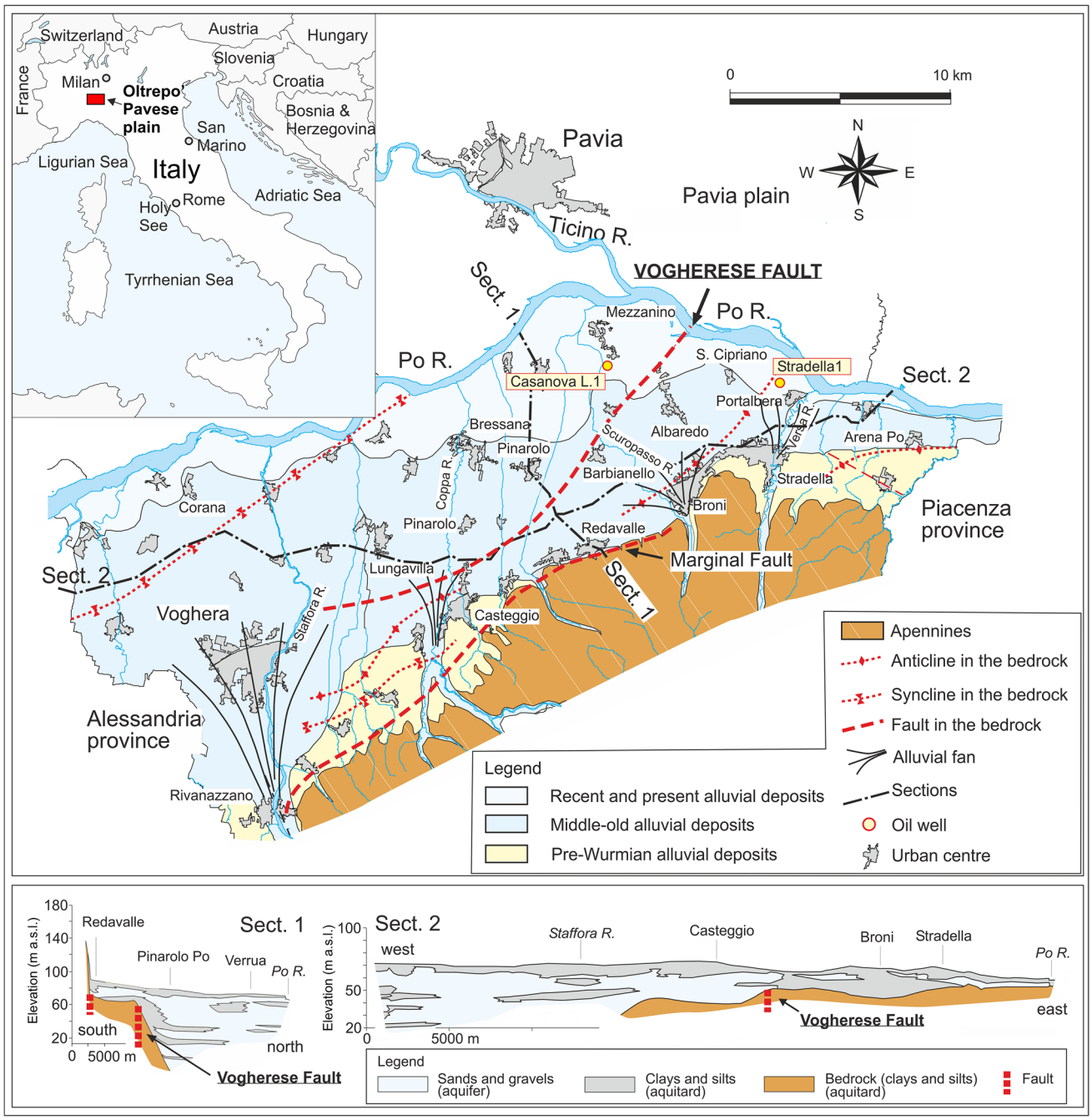

Fig. 1 Geographical and geological setting of the Oltrepò Pavese plain sector in northern Italy, with hydrogeological sections (simplified from Cavanna et al. 1998). At the studied area, the alluvial aquifer is strongly conditioned by the presence of an important tectonic discontinuity, the Vogherese Fault, along which the saline waters are mainly distributed and which is responsible for the sudden deepening that affects the hydrogeological bedrock (sections). The uplift of the bedrock to the south-east of the Vogherese Fault (sections) is related to the Apennines uplift. Figure modified from Torrese and Pilla (2021)

strong variability on the thickness of the aquifer. The aquifer shows a thickness of a few meters in the southern sector, that represents the upper block, and hundreds of meters in the northern sector, the lower block (Braga and Cerro 1988; Cavanna et al. 1998; Regione Lombardia and ENI Divisione AGIP 2002; AGIP 1972; Fig. 1).

There are two deep boreholes (500 m) in the area drilled for oil exploration (AGIP 1972; Regione Lombardia and ENI Divisione AGIP 2002) (Fig. 1). The Casanova Lonati 1 borehole (Fig. 1), which is located on the down-lifted block of the Vogherese Fault, intercepts the underlying marine deposits at a depth of 275 m. Brackish groundwater, which rises along

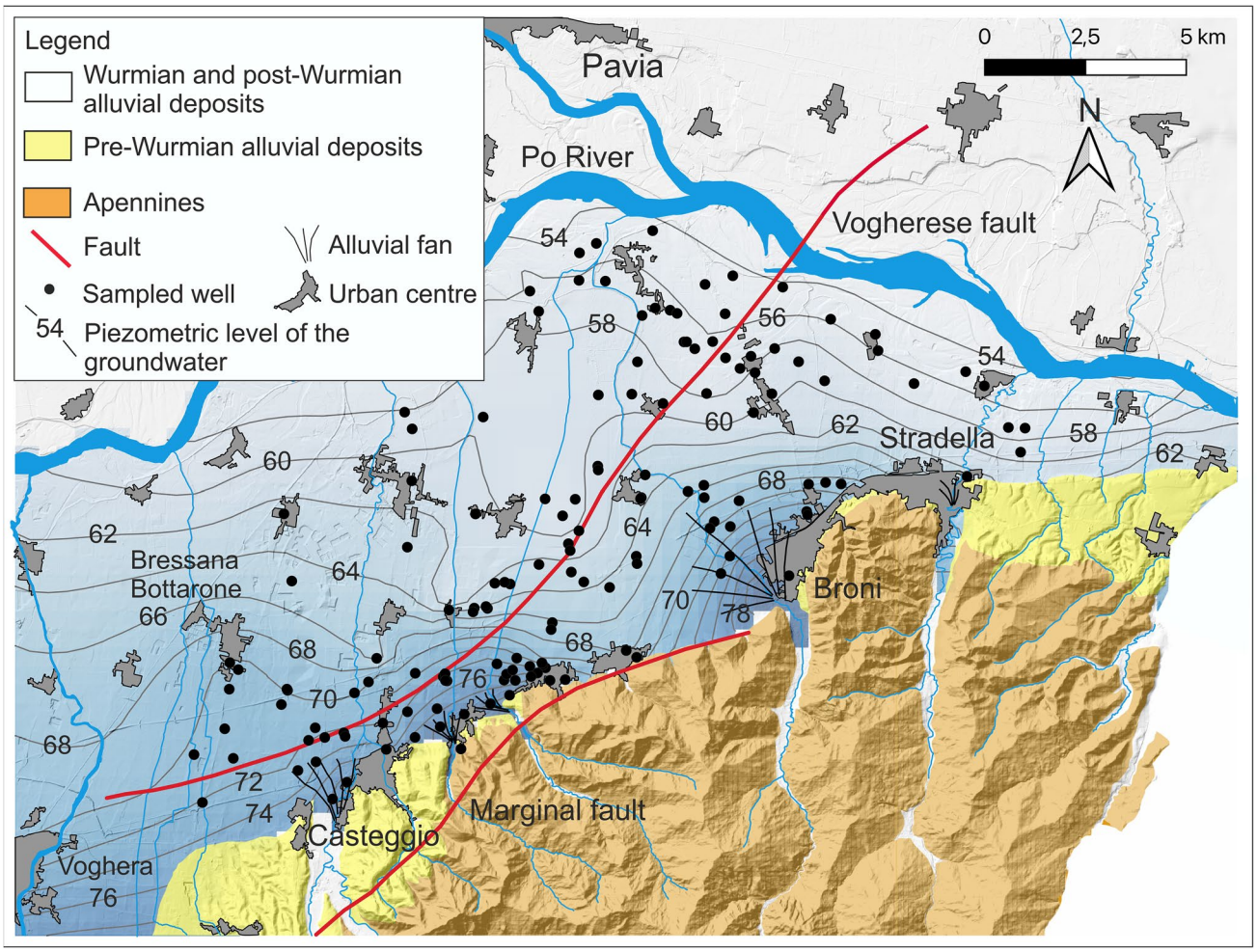

Fig. 2 Piezometric levels of groundwater in the shallow aquifer, June 2005

the fault and flows into the continental deposits, is intercepted by the borehole at 136 m. Groundwater intercepts salt waters at 400 m, as revealed by self-potential and resistivity logs, as well as formation testing. Formation tests found Na–Cl up to a concentration of 34.4 g/L in the bedrock at depths of several hundred meters. The second borehole, the Stradella 1 borehole (Fig. 1), located on the up-lifted block of the fault, intercepts the underlying marine deposits at a depth of only 36 m.

This particular setting facilitates the phenomenon of uprising saline waters which appears most prominently in the southern sector of the plain where the aquifer is thinner. Here the Na–Cl-rich waters cannot be diluted by the more abundant calcium-bicarbonate (Ca–HCO_3) groundwaters. This outlined setting strongly influences the chemistry of the groundwater. The origin of the Na–Cl-rich waters is connected to the brines (very high-density fluids) that are remnants of evaporated marine waters in the late Messinian, trapped at the bottom of the Po plain aquifer (Conti et al. 2000; Regione Lombardia and ENI Divisione AGIP 2002). The uprising of saline waters is also facilitated by structural discontinuities localized in the bedrock of marine origin. These discontinuities represent preferential flow paths for the saline waters and facilitate the flow towards the alluvial aquifer.

The existence of these mineralised waters in the Oltrepò Pavese area has been well known since Roman times. In fact, the waters were (and still are) exploited for thermal purposes (S. Colombano al Lambro, Miradolo Terme, Salice Terme and Rivanazzano Terme are the most famous Spa centres located near the investigated area). The investigated area of the Oltrepò Pavese plain sector shows a fully flat topographical surface.

Materials and methods

Hydrochemical investigations

The hydrogeochemical study included the periodical sampling and analysis of 146 wells drilled in alluvial deposits.

These wells are mainly used for agricultural purposes and most are located close to the Vogherese Fault (Fig. 3). The maximum depth of the sampled wells typically varies between 10 and 20 m, all the wells are fully screened, and the well samples were taken at half of the maximum well depth.

The sampling was carried out between July 2007 and July 2013. Hydrogeochemical characteristics, groundwater levels, in situ temperature (T), electrical conductivity (EC), redox potential and pH were monitored. The variation in the degree of water salinity with depth and the freshwater/saltwater interface were also monitored through vertical logs of EC and T that were carried out from July 2008 on 63 wells.

Major ions were analyzed in the laboratory of Università di Pavia with a Dionex DX 120 chromatograph, while volumetric analysis was used for the determination of alkalinity. A Pasi BFK 100 hydrostatic probe was used for measuring piezometric levels, a WTW LF597 conductivity meter was used for acquiring electrical conductivity and temperature data, and a WTW pH 340/ION was used for acquiring pH

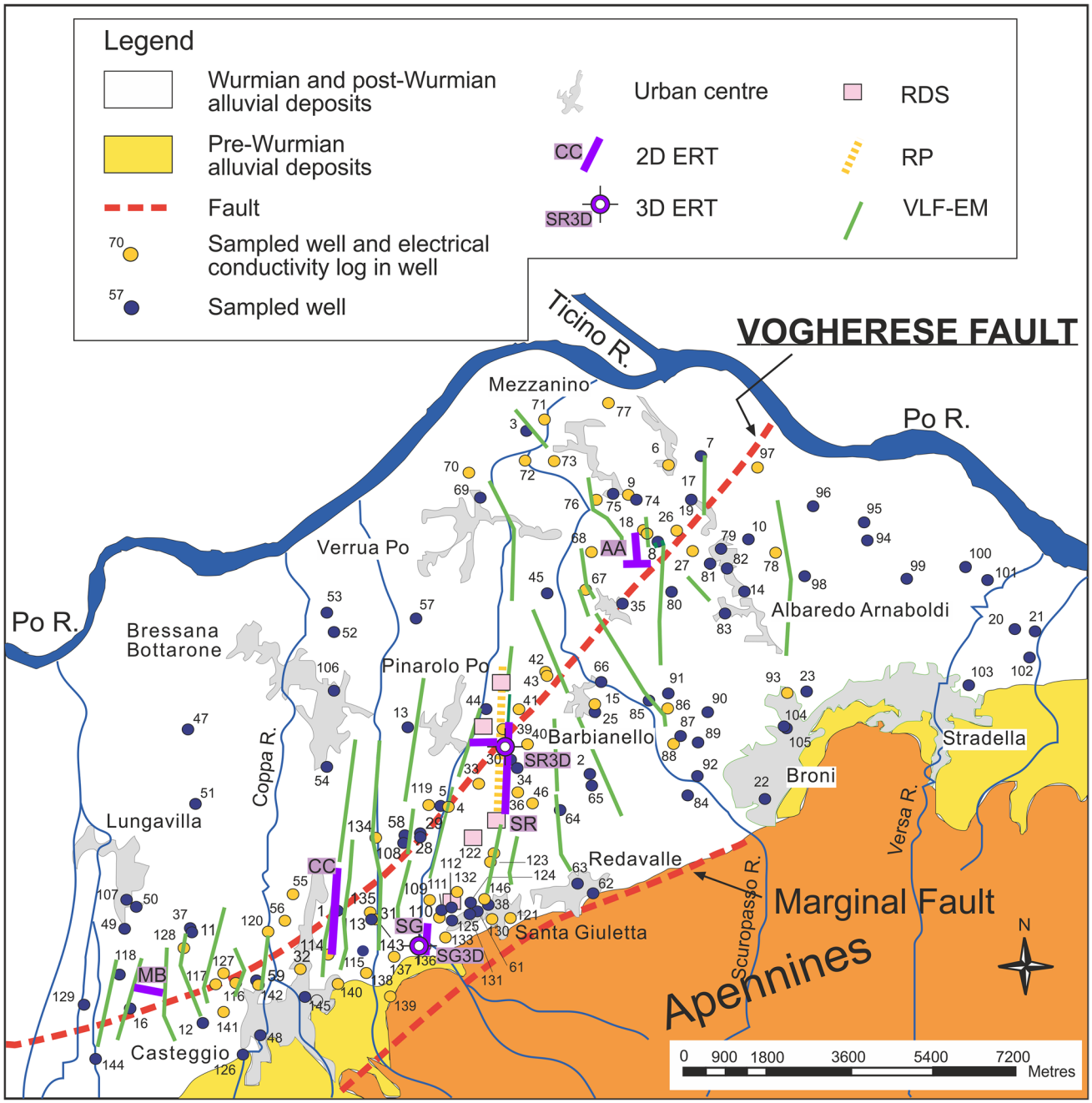

Fig. 3 Investigations undertaken in the studied area

and Redox potential data. Groundwater sampling from the wells was carried out with submersible electric pumps supplied with the well, a Cellai 504S peristaltic pump, or with a bailer.

Geophysical investigations

Geophysical investigations were undertaken in three separate phases, whereby the first two were preliminary investigations while the third was a more detailed investigation. During the first phase, 17 RDS's were undertaken along a cross section of the Vogherese Fault with the objective of reconstructing the geometry of the bedrock and the different hydrogeological units. These were undertaken in a subarea that is considered representative of the entire study area and were necessary for the calibration of the investigations for the following phases.

The second phase involved VLF-EM surveys carried out over vast areas for a rapid assessment of the distribution of saline waters within the aquifer, even in those areas where no wells for sampling are available. In all, 35 profiles (Fig. 3) were undertaken over an area of approximately 150 km^2 along the Vogherese Fault, using a WADI instrument by ABEM™. Both north–south and northwest–southeast profiles were undertaken with a spatial sampling of 10 or 20 m.

The third, more detailed phase of the investigations, was carried out at test sites selected on the basis of the observations from the first two phases, and involved:

- A resistivity profile, 2,160 m in length, crossing the Vogherese Fault in a N–S direction and overlapping with a VLF-EM profile (test site SR in Fig. 3)
- Five RDS's aimed at a localized calibration of the other geophysical surveys (test site SR in Fig. 3)
- A transect composed of five two-dimensional (2D) ERT's, approximately 2,600 m long, crossing the Vogherese Fault and partially overlapping with the resistivity profile (test site SR in Fig. 3)
- A transect composed of four 2D ERT's (surveys CC1-CC4), approximately 1,880 m long, undertaken in a saline-water contaminated area (test site CC in Fig. 3)
- Five 2D ERT's (test sites AA, MB, SG and SR in Fig. 3), 470 m long each, two of which were roughly orthogonal to each other (test site AA in Fig. 2, AA1 and AA2)
- Five 3D ERT's (test sites SG and SR in Fig. 3), with a surface grid 110 m × 30 m in size each, for an accurate investigation of localized brackish-water plumes contaminating the alluvial aquifer

Each ERT profile is 470 m in length and was obtained using 48 electrodes spaced 10 m apart. Each 3D ERT involved a surface snake grid comprised of 12 × 4 electrodes spaced 10 m apart both along the X and Y axes. A fully automatic multielectrode resistivity meter, SYSCAL Jr. Switch-48 by IRIS Instruments (400 V max output voltage, 1200 mA max output current, 100 W max output power), was used for acquiring all electrical resistivity data.

Among the geophysical surveys carried out in the area, this paper reports the results obtained from some 2D and three-dimensional (3D) ERT surveys: a long transect (CC1-CC4 in Fig. 3) to define the hydrogeological setting of the area and detailed surveys (AA1, AA2, SG3D and SR3D in Fig. 3) to investigate localized zones of the aquifer affected by saline-water contaminations.

ERT data inversion was performed using ERTLab Solver (Release 1.3.1, by Geostudi Astier s.r.l. - Multi-Phase Technologies LLC) based on tetrahedral finite element modelling (FEM). Tetrahedral discretization was used in both forward and inverse modelling and in both 2D and 3D ERT's (even 2D models were obtained from 3D inversion). The foreground region was discretized using a 5-m cell size for all 2D and 3D ERT's, i.e., half the electrode spacing, to give the model high accuracy. The background region was discretized using an increasing element size towards the outside of the domain, according to the sequence: 1×, 1×, 2×, 4× and 8× the foreground element size.

The forward modelling was performed using mixed boundary conditions (Dirichlet-Neumann) and a tolerance (stop criterion) of 1.0E-7 for a symmetric successive over-relaxation conjugate gradient (SSORCG) iterative solver. Data inversion was based on a least-squares smoothness constrained approach (LaBrecque et al. 1996). Noise was appropriately managed using a data-weighting algorithm (Morelli and LaBrecque 1996) that allows the variance matrix after each data point iteration that was poorly fitted by the model to be adaptively changed. The inverse modelling was performed using a maximum number of internal inverse preconditioned-conjugate-gradient (PCG) iterations of 5 and a tolerance (stop criterion) for inverse PCG iterations of 0.001. The amount of roughness from one iteration to the next was controlled to assess maximum layering: a low value of reweight constant (0.1) was set with the objective of generating maximum heterogeneity.

Inversion involved the application of homogeneous starting models with the average measured apparent resistivity. The final inverse resistivity models were chosen based on the minimum data residual (or misfit error).

Cross-validation of geophysical results with well logs

Vertical logs were carried out in shallow water wells, used for irrigational purposes, available at the site (Fig. 3). These wells were drilled prior to the present study, with destructive

rotary or auger techniques until the top of the (impermeable) bedrock. All the wells are fully screened. Although no logs of chip samples are available and these wells do not provide accurate stratigraphic logs, they still provide information regarding the depth to bedrock below alluvial deposits, which was helpful in interpreting geophysical models. The paper shows a comparison between well logs carried out in well 30 and 3D geophysical results. This well, which is located in the southern sector with respect to the Vogherese Fault trace (Fig. 3), provided an ideal opportunity to cross-validate detailed geophysical results with ground truth. Well 30 intercepts the transition between slightly brackish groundwater and underlying moderate brackish groundwater at 11 m depth. This made it possible to define the representative resistivity range for different degrees of salinity of groundwater saturating the alluvial deposits. In this study, water salinity was classified according to these classes: freshwater with EC < 500 µS/cm, slightly brackish water with EC ranging between 500 and 4,000 µS/cm, moderately brackish water with EC ranging between 4,000 and 8,000 µS/cm, highly brackish water with EC ranging between 8,000 and 12,000 µS/cm, salt water with EC ranging between 12,000 and 70,000 µS/cm, brine with EC > 70,000 µS/cm. The term 'saline water' is used to define a highly mineralized water and includes both brackish water and salt water.

Results

Hydrochemical results

Two main hydrochemical facies can be identified within the Oltrepò Pavese groundwater: a Ca–HCO_3 hydrofacies, which characterises most of the groundwater of the Oltrepò Pavese alluvial aquifer; a Na–Cl hydrofacies, which locally characterises the groundwater in some sectors of the Oltrepò Pavese area along the Vogherese Fault (Fig. 5).

The Ca−HCO_3 hydrofacies has low-to-medium mineralization with electrical conductivity ranging between 800 and 1,200 µS/cm and chloride concentration between 2 and 200 mg/L. The Na–Cl waters have a high degree of mineralization with electrical conductivity that often exceeds 20,000 µS/cm and chloride concentration ranging between 200 and 12,000 mg/L. Na–Cl waters have an extremely variable degree of mineralization over the area (Figs. 5 and 6). This variability is associated with the different degrees of mixing between the shallower groundwater and the deeper saline waters (brines of the Po Plain). Evidence of this variability is represented at the surface with the thermo-mineralised springs at Salice Terme, Rivanazzano Terme and San Colombano Terme (Figs. 5 and 6).

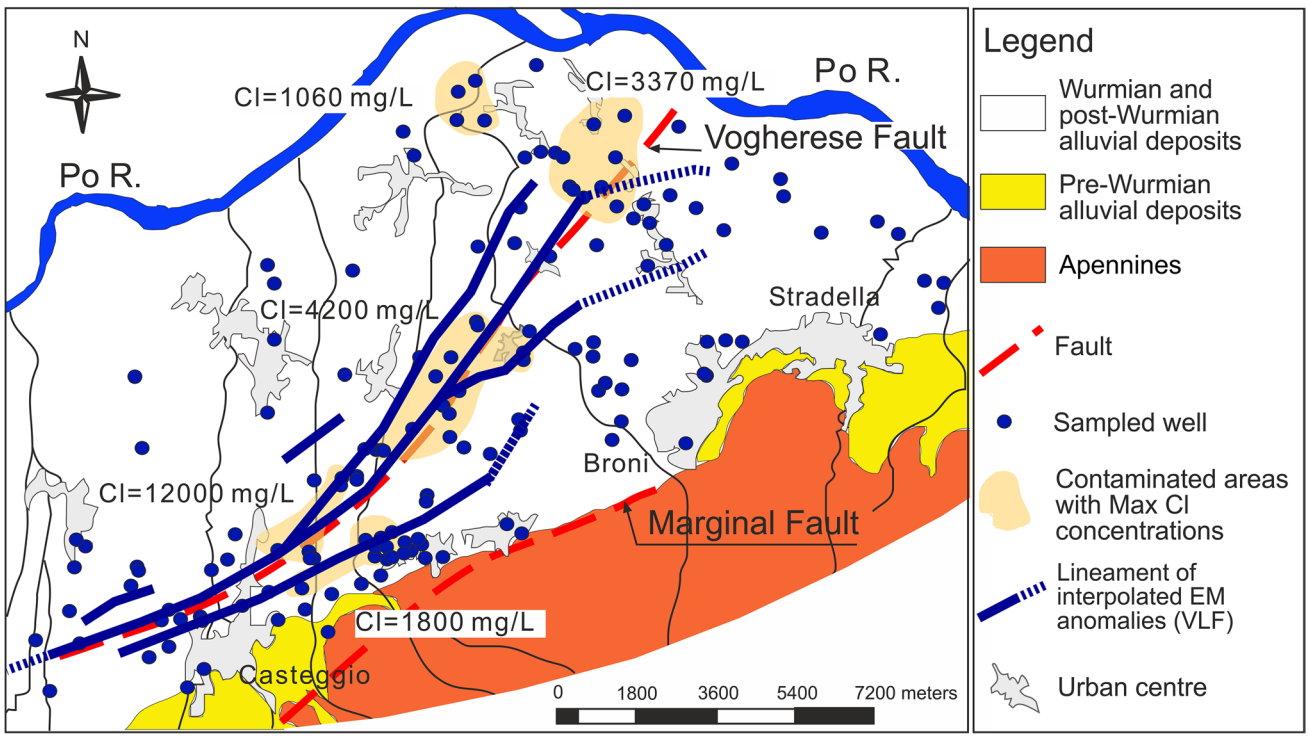

Fig. 4 Most chloride-contaminated zones of the Oltrepò Pavese aquifer, with reference to the Vogherese Fault trace and to the main NE–SW trends of high-conductivity anomalies revealed by VLF-EM surveys which can be correlated with the up-rise of mineralized waters along secondary tectonic discontinuities

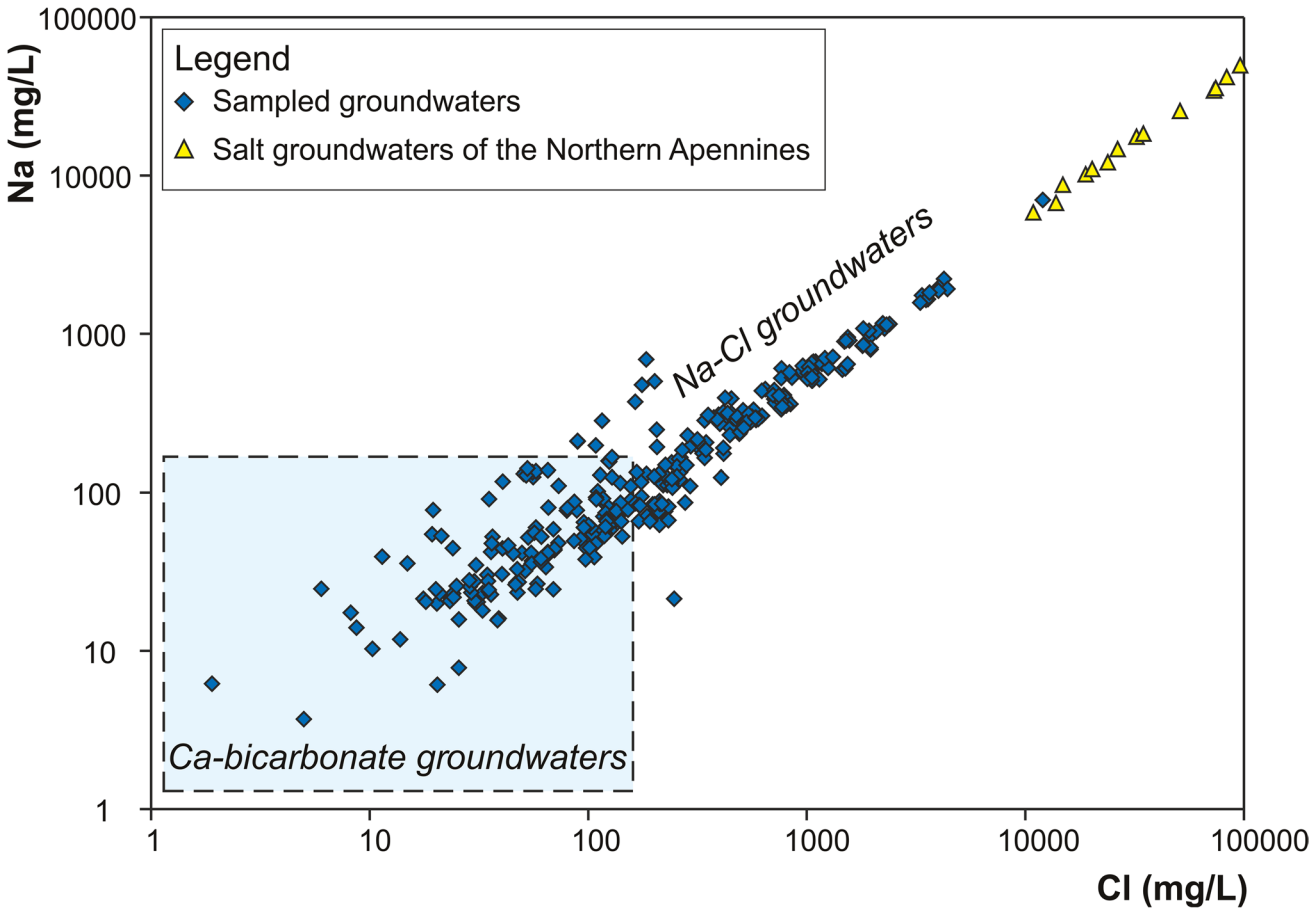

Fig. 5 Na versus Cl diagram from sampled waters. Salt waters of the northern Apennines from Bersan et al. (2007) and Boschetti et al. (2011)

Undesirable metals, like iron, manganese, arsenic and selenium, represent another peculiarity of the Oltrepò Pavese groundwater (Pilla et al. 2007). These metals, which compromise the quality of the waters even more, frequently accompany the already high chloride and sodium concentrations, often above the Italian drinking-water standards —250 mg/L for chloride; 200 mg/L for sodium (Italian Legislative Decree, Decreto Legislativo 2 febbraio 2001, n. 31, Italian Legislature 2001).

The Ca–HCO_3 waters in the Oltrepò Pavese area are characterised by chloride values that do not exceed 200 mg/L; concentrations of bicarbonate vary between 300 and 700 mg/L, calcium varies between 50 and 200 mg/L, magnesium varies between 30 and 50 mg/L, and sulphates vary between 30 and 100 mg/L.

The Na–Cl groundwater has a significantly higher mineralization (EC values can be above 12,000 µS/cm and is on average between 2,000 and 5,000 µS/cm, Fig. 6). The EC values are related to the solubilised chloride and sodium, given that the concentrations of other major ions are relatively similar to those of the Ca–HCO_3 water described earlier. Well 15 at Barbaniello (Fig. 3) is the only exception. The EC values recorded at this location, sometimes above 5,000 µS/cm, are mainly connected to the high sulphate concentrations that vary between 800 and 2,700 mg/L. The origin of this calcium-sulphate groundwater can be connected to evaporite layers within the Gessoso-Solfifera Formation which are present locally at the base of the Oltrepò Pavese aquifer (Bersan et al. 2010).

Hydrochemical investigations have shown three areas along the Vogherese Fault where the phenomenon seems to be more intense and widespread: the area to the north of Casteggio where the chloride can exceed 10,000 mg/L; the area to the west of Barbianello where the highest concentrations (above 4,000 mg/L) of chloride were recorded, and finally, the sectors that includes Mezzanino and Albaredo Arnaboldi, where chloride concentrations can reach 3,000 mg/L (Fig. 4).

While the distribution of the Na–Cl groundwater is controlled by the trend of the Vogherese Fault at a regional scale (Fig. 4), higher variability in the distribution of the saline groundwater is observed at a local scale within the aquifer (Fig. 6). The chloride concentrations mentioned earlier are the highest measured concentrations for each of

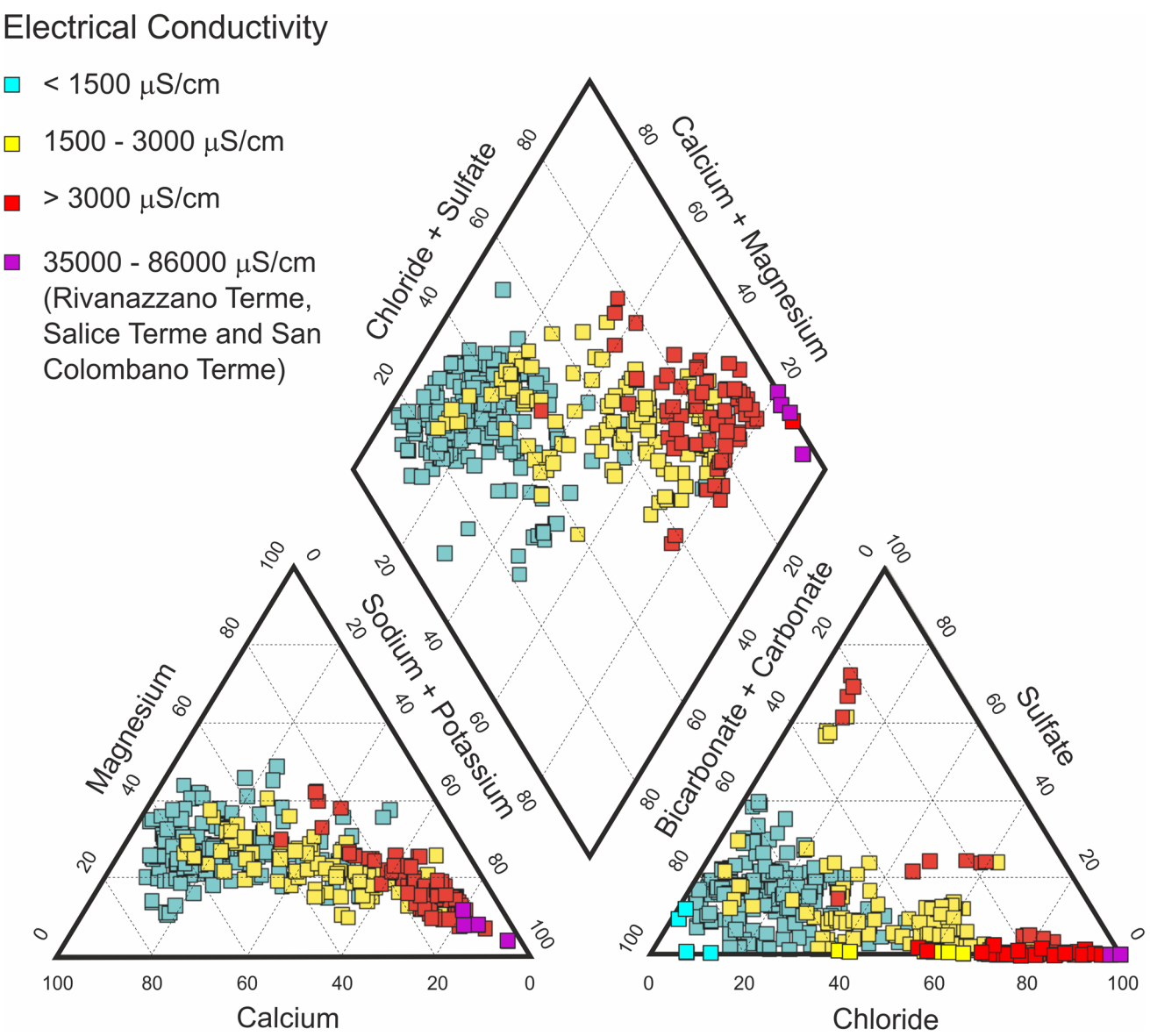

Fig. 6 Piper diagram, including electrical conductivity, from sampled waters

the areas. However, groundwater with lower concentrations (300–400 mg/L) was sampled in nearby wells, which is indicative of ongoing natural contamination, although with different intensities. The correlation between the chemistry of the aquifer and the trend of the Vogherese Fault is not always observed. Some wells, although close to the fault, show low mineralization of the groundwater (wells 32, 34 and 35).

The investigations that were undertaken for some sectors of the studied area allowed identification of the transition zone between the shallow fresh groundwater and the heavily mineralised deep groundwater (Fig. 7). In general, groundwater salinity starts to increase at depths of between 5 and 8 m, which can increase to depths of 10–20 m. In other cases, the depth is just below ground level, like in some subareas of the studied area where saline waters were found in the surface drainage network which is buried in the first few metres of the drift deposits (Bersan et al. 2010). Acquired data show that groundwater above and below the transition zone does not show the same degree of mineralization. This indicates that the intrusion of saline waters within the aquifer is not evenly distributed within the study area (Fig. 8). A strong increase of salinity with depth (EC increased from 3,000 to approximately 14,000 µS/cm) was recorded in some wells (well 27), while salinity was less variable (within a few thousand µS/cm) along the vertical of other wells.

Neither the Ca–HCO_3 waters nor the Na–Cl waters show the same electrical conductivity within the different

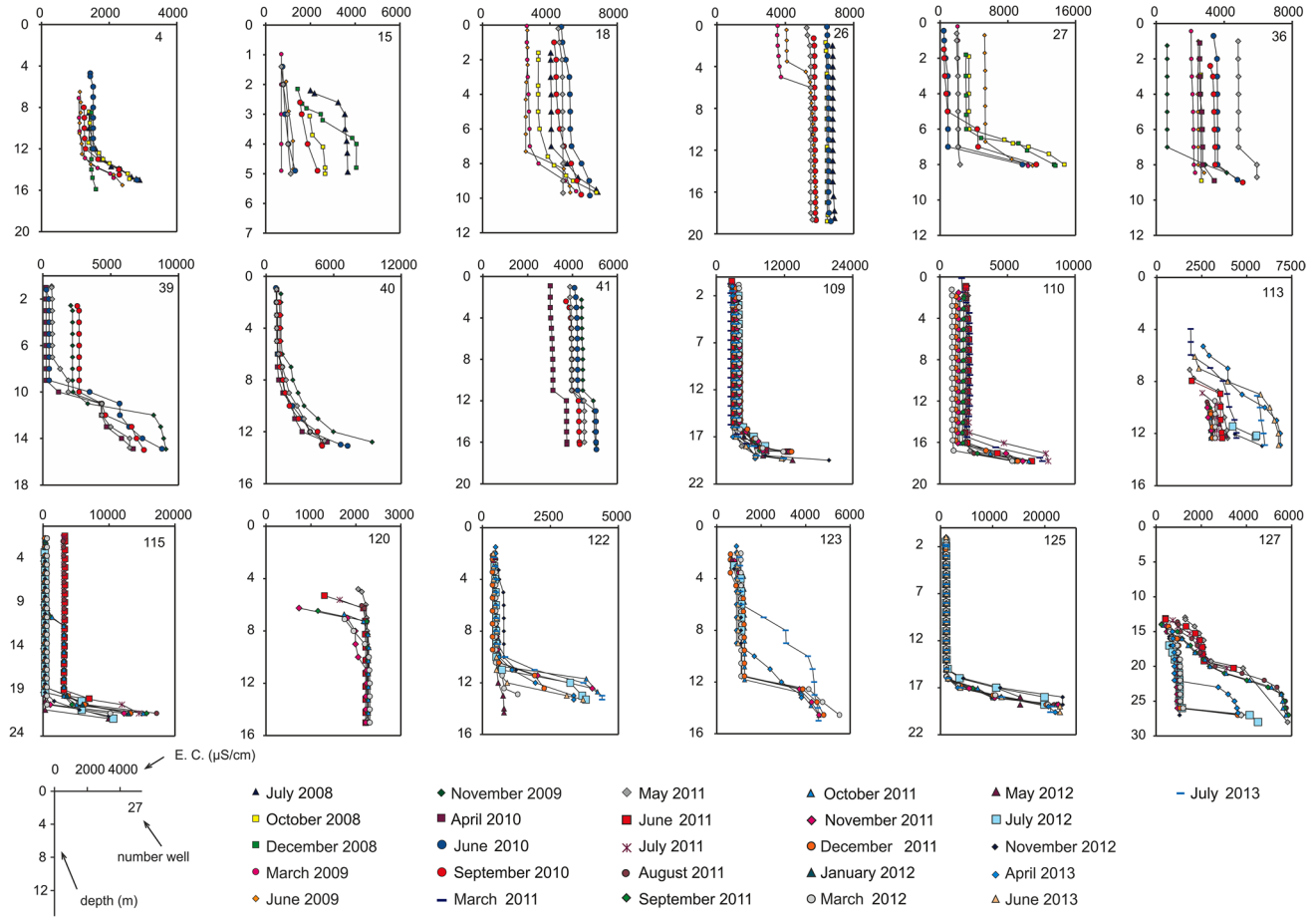

Fig. 7 Electrical conductivity logs undertaken within some of the monitored wells

areas of the plain. In some sectors, groundwater shows electrical conductivity values between 2,000 and 6,000 µS/cm (wells 18, 26, 27, 36, 39, 41, 109, 113, 115, 120) even over the transition zone, in place of freshwaters. Into the transition zone, the electrical conductivity of waters varies between 2,500 and 10,000 µS/cm, depending on the area, while, below the transition zone, values between 3,000 and 23,000 µS/cm were detected—Table S1 in the electronic supplementary material (ESM).

This particular context is well illustrated by Fig. 8, which shows the distribution of wells with logs across the Vogherese Fault, their depth, and the maximum values of electrical conductivity ever measured for groundwater both at the top and at the bottom of wells. One can observe that the majority of wells characterized by the highest values of electrical conductivity (red ones) are located within a distance of 1.5 km in the southern sector and of 1 km in the northern sector from the Vogherese Fault. One can also notice the presence of a few contaminated wells very far from the fault (about 4 km), both in the northern and in the southern sector. They are probably connected to the existence of secondary tectonic discontinuities that convey deep salt-water into the alluvial aquifer. Moreover, into the most contaminated zone (<1 km), wells are not all contaminated by chloride, but some of them are characterized by low values of electrical conductivity (<1,500 µS/cm up-well; <2,000 µS/cm down-well).

Geophysical results

Phase 1 of the investigations (RDS) has shown that the hydrogeological bedrock at the base of the continental deposits is deeper in the northwestern areas and is also characterized by morphological irregularities (small troughs and/or peaks), partly shaped by tectonics and partly shaped by the Scuropasso and Versa paleo-rivers.

Phase 2 of the investigations (VLF-EM) has shown that a main NE–SW trend of high-conductivity anomalies was revealed at a large scale (Fig. 4). This trend can be correlated to the occurrence of the Vogherese Fault trace and therefore it can be correlated with the up-rise of mineralized waters along the fault zone. At least one secondary NE–SW alignment of high-conductivity anomalies

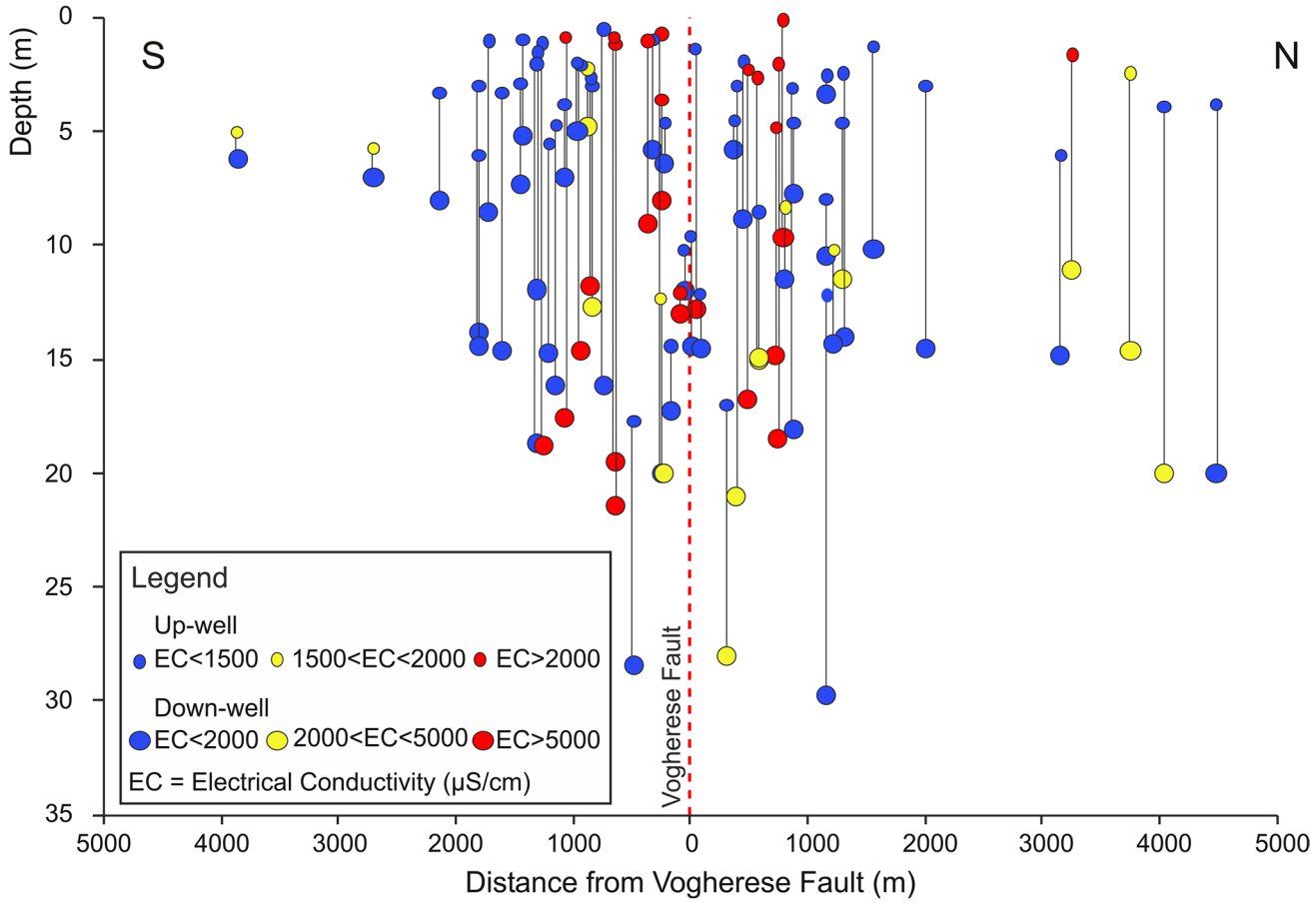

Fig. 8 Distribution of wells with logs across the Vogherese Fault, their depth and the maximum values of electrical conductivity ever measured for groundwater both at the top and at the bottom of wells

is shown. Other NE–SW minor trends were also identified, suggesting the existence of secondary and subparallel discontinuities (Fig. 4). These results indicate that the uprising mineralised waters that originate from the Mio-Pliocene deposits contaminate the superficial aquifer in correspondence of several subparallel discontinuities oriented in a NW–SW direction.

The hydrogeological configuration revealed by phases 1 and 2 is confirmed by the more accurate and complete phase 3 of the investigations. In 2D ERT inverse resistivity models (Figs. 9 and 10), warm colours (from green to red) are associated with freshwater-saturated or brackish-water-saturated alluvial deposits (e.g., freshwater-saturated clayey-to-sandy deposits or brackish-water-saturated sandy deposits); cool colours (blue) are associated with clayey and silty cover deposits, saline-water-saturated alluvial deposits (e.g., saline-water-saturated sandy-to-gravelly deposits) or with the clayey bedrock (locally saline-water saturated). The inverse models indicate sharp and irregular contact between the alluvial aquifer and the underlying hydrogeological bedrock. The hydrogeological bedrock (3–6 Ω·m) at the base of the alluvial aquifer (20–40 Ω·m) is characterized by morphological irregularities, which are likely to have been shaped either by tectonics (Vogherese Fault zone) and/or by the paleo-river's erosion. In the southern area of the investigated transect (south of the fault) the thickness of the aquifer varies between 10 and 30 m (Figs. 9 and 10). This depth increases northward due to the Vogherese Fault (Figs. 9 and 10). These evidences are consistent with well observations regarding bedrock depth. ERT results allowed for detailed localization and trace of the Vogherese Fault in the investigated area.

The complexity of the geometry of the areas where the high-salinity groundwater is found in proximity to the fault was also identified at the local scale within this phase of the investigations. The bedrock is affected by saline-water contamination which shows resistivity values lower than 5 Ω·m (Figs. 9 and 10). These areas of contamination are likely localized along structural discontinuities which represent preferential flow paths for the saline waters and facilitate the flow towards the alluvial aquifer.

The resistivity imaging revealed an extremely variable salinization within the aquifer (according to Torrese

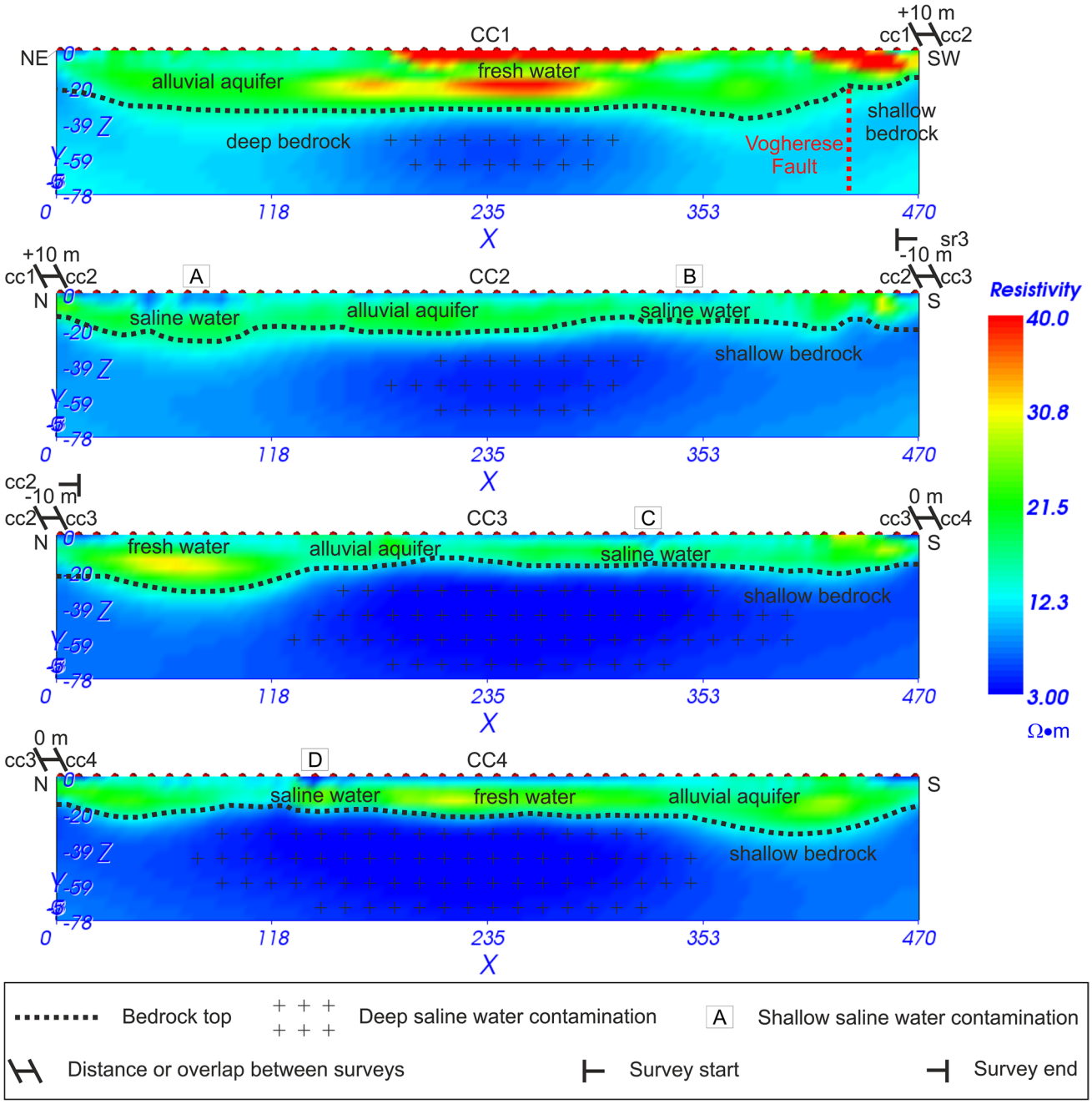

Fig. 9 ERT transect (CC; approximately 1,880 m long) which shows the geometry of the bedrock at the base of the alluvial aquifer, its sudden deepening towards the north-western sector of the plain due to the presence of the Vogherese Fault (CC1) and the occurrence of localized and restricted zones of salinization within the aquifer

and Pilla 2021) over the investigated area. Low-resistivity anomalies (cool colors within the aquifer) are found in correspondence of saline-water contamination; high-resistivity anomalies (warm colors within the aquifer) are found in correspondence of contamination-free zones (Figs. 9 and 10). The variability of electrical resistivity with depth is associated with the different degrees of mixing between the shallower fresh groundwater and the deeper saline waters (brines of the Po Plain). No correlation was observed between the variation in the degree of salinity of the water and the piezometric level of the groundwater.

While the distribution of the Na–Cl groundwater is controlled by the trend of the Vogherese Fault at a regional scale (Fig. 4), higher variability in the distribution of the saline groundwater is observed at a local scale within the aquifer. Both the 2D and 3D ERT (Figs. 9, 10, 11 and 12)

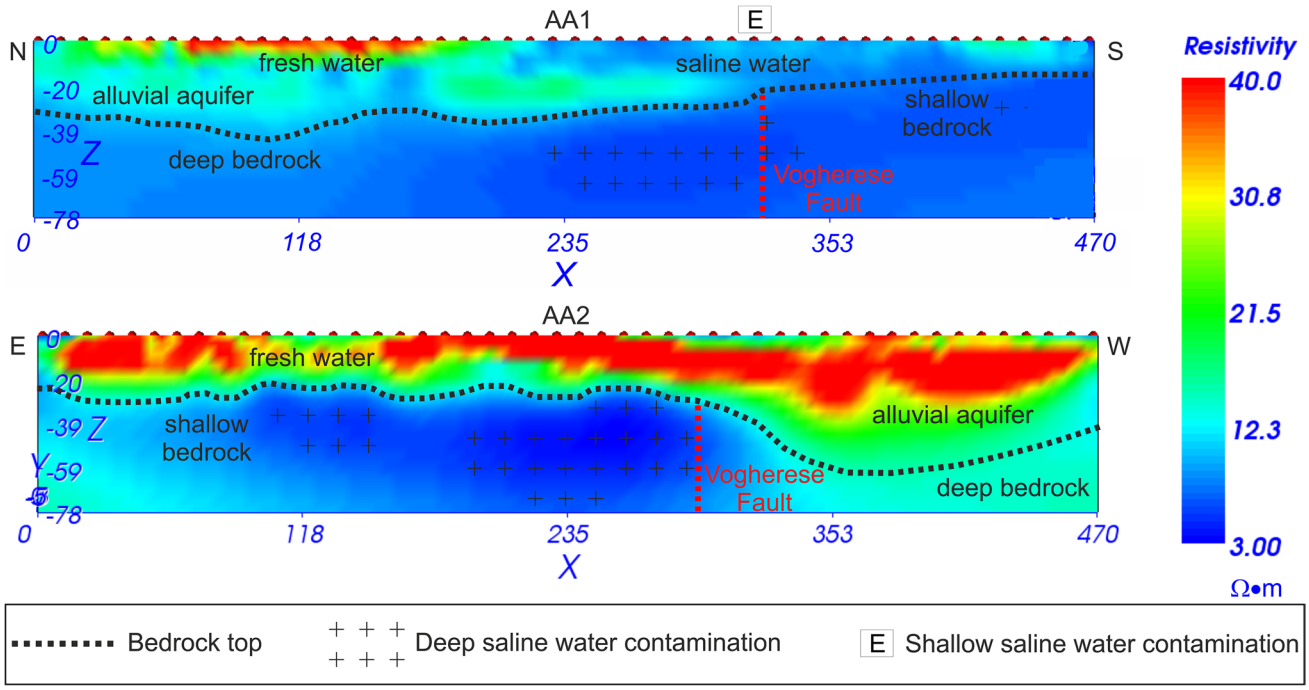

Fig. 10 Two-dimensional ERT models (AA) which show the geometry of the bedrock at the base of the alluvial aquifer, its sudden deepening towards the north-western sector of the plain due to the presence of the Vogherese Fault (AA1), the occurrence of localized and restricted zones of salinization within the aquifer (E), and a large portion of the alluvial aquifer free from saline-water contaminations (AA2)

surveys pointed out the existence of localized and restricted zones of the aquifer affected by saline-water contamination which are likely localized along structural discontinuities (A–E in Figs. 9 and 10). These zones show resistivity values ranging between 3 and 8 Ω·m. These contamination-related low-resistivity anomalies correspond to high-amplitude anomalies identified along the VLF-EM profiles.

Three-dimensional ERT's provided a detailed 3D imaging of the irregular-shaped shallow salt-water-to-brackish water plumes contaminating the alluvial aquifer (Figs. 11 and 12). Here, deep saline waters, which reach the alluvial aquifer during upward migration, diffuse and mix with the fresh groundwater of the shallow aquifer, therefore originating different degrees of groundwater salinity within the aquifer. Salt-water-to-brackish waters are associated with bulk resistivity values lower than 12 Ω·m in SG3D (Fig. 10) and lower than 9.3 Ω·m in SR3D (Fig. 12). Slightly brackish waters to freshwaters are associated with bulk resistivity values ranging between 30 and 78 Ω·m (Figs. 11 and 12).

Comparison between geophysical results and well logs

When analysing the resistivity log (EC log) undertaken on the 5th June 2013, which was used for the cross-validation of SR3D geophysical survey (Fig. 12), a transition can be found between slightly brackish groundwater (1,430 µS/cm on average, 1–10 m of depth, June 2013) and underlying moderate brackish groundwater (5,262 µS/cm on average, 11–15 m of depth, June 2013) at 11 m depth. Likewise, the temperature log (5 June 2013, Fig. 12) shows a transition between shallower relatively colder groundwater (average temperature of 12.8 °C, 3–10 m of depth, June 2013) and deeper relatively warmer groundwater (average temperature of 13.5 °C, 11–15 m of depth, June 2013) at 11 m depth.

The drop in resistivity (EC log) found at 11 m depth, along with an increase of temperature and a decrease of redox potential of groundwater, are well correlated to the presence of a salt-water-to-highly-brackish water plume (resistivity lower than 9.3 Ω·m) revealed by the geophysical model (Fig. 12a). This well transition zone occurs in a portion of the aquifer in which, based on the bulk resistivity indicated by the ERT survey, the aquifer should be characterized by clean sands deposits.

At shallower depths, the presence of slightly brackish to fresh groundwater is well correlated with higher resistivity values revealed by the geophysical model (Fig. 12b). Based on the bulk resistivity (resistivity higher than 30 Ω·m), the geophysical model suggests the presence of finer deposits saturated with slightly brackish groundwater. This suggests that the distribution of saline-water contamination areas is a

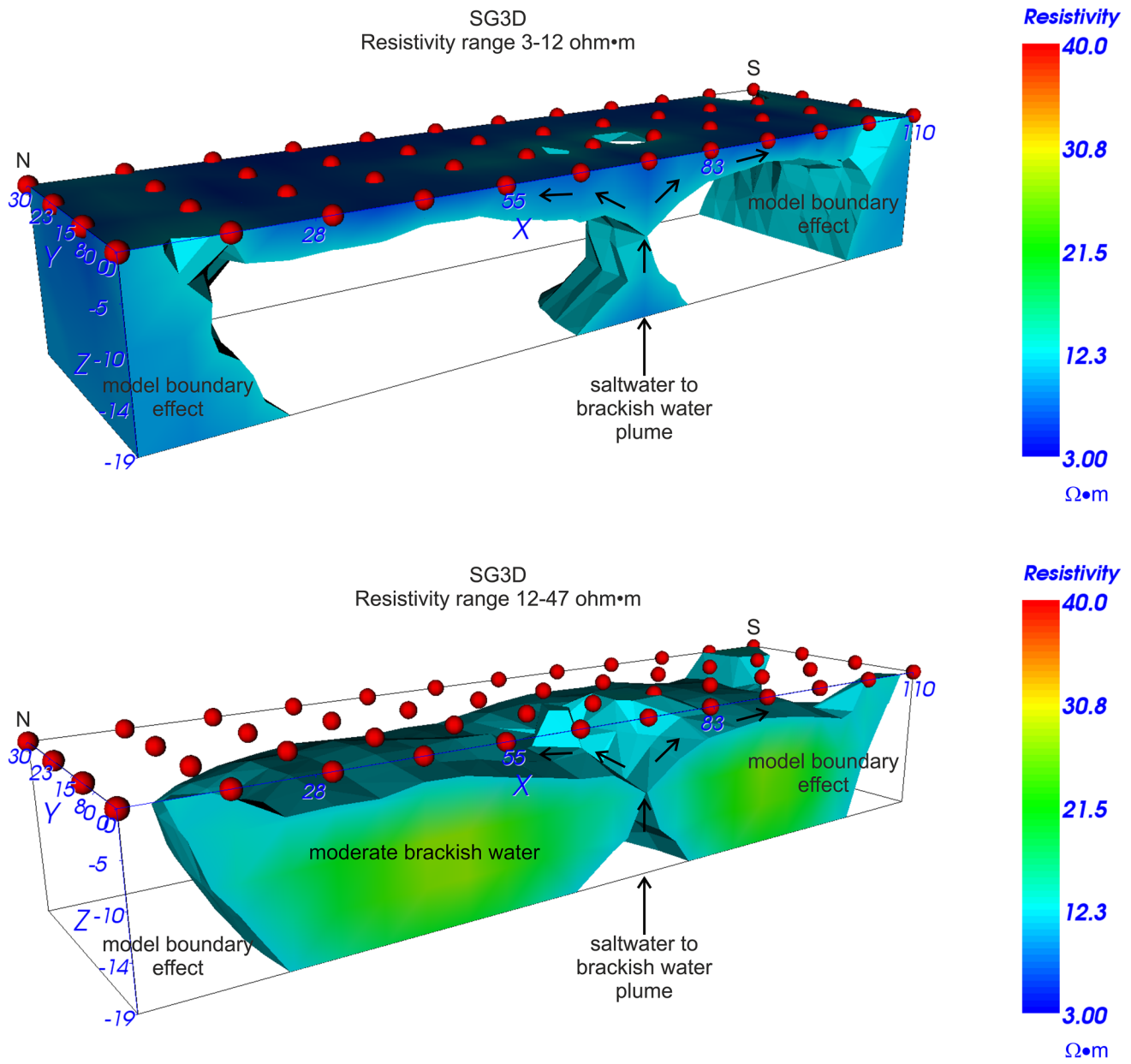

Fig. 11 Three-dimensional ERT model (SG) which shows a saltwater-to-brackish water plume (3–12 Ω·m) contaminating the alluvial aquifer (12–47 Ω·m): deep saline waters reach the alluvial aquifer during upward migration, then diffuse and mix with the fresh groundwater of the shallow aquifer

hydraulic-conductivity-controlled process at the plume scale within alluvial deposits.

Discussion

The study enabled definition of the general hydrogeological setting of the investigated area, as well as detailed investigation of localized and restricted zones of the aquifer which are crucial elements for the understanding of the saline-water contamination process and the exploitation management of the aquifer.

Sharp and irregular contact between the alluvial aquifer and the underlying bedrock was observed. The bedrock is characterized by morphological irregularities, which are likely to have been shaped either by tectonics (Vogherese Fault zone) and/or by the paleo-river's erosion. Although, in the southern investigated area (south of the fault) the thickness of the aquifer varies between 10 and 30 m, the bedrock depth increases northward due to the Vogherese Fault. These evidences are consistent with well observations regarding

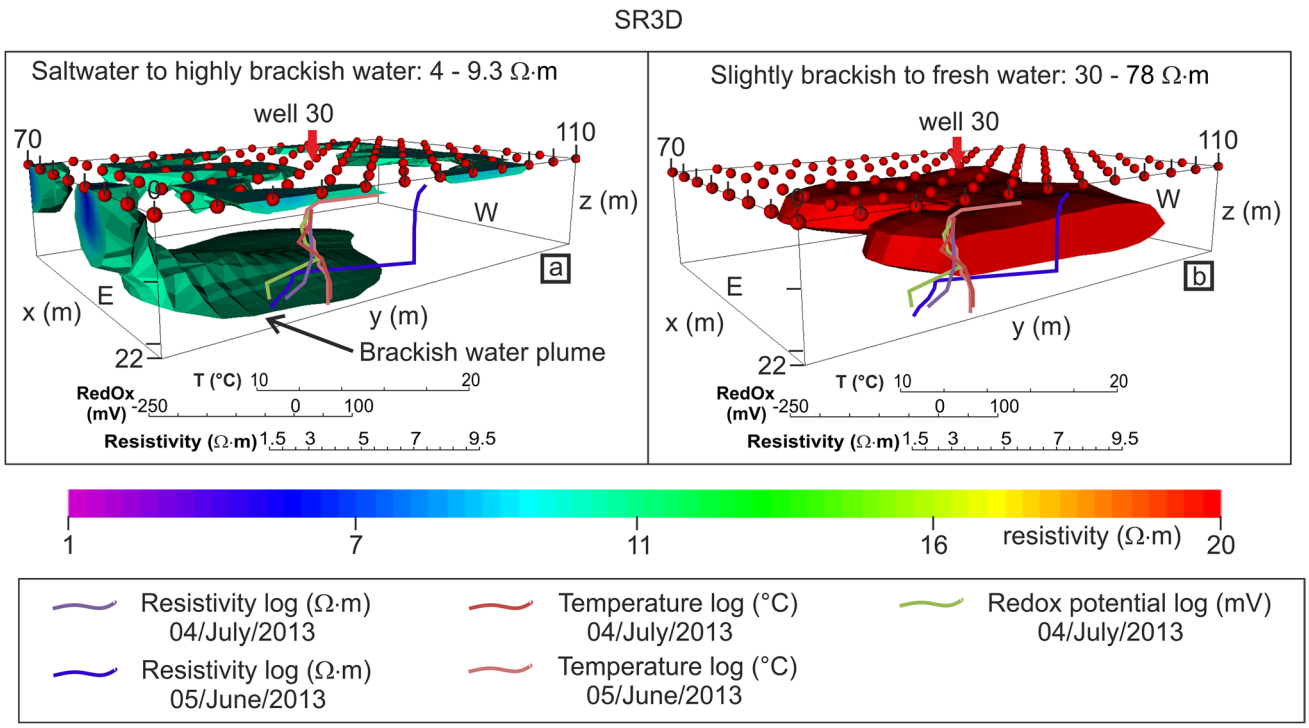

Fig. 12 Three-dimensional ERT model (SR) cross-validated with well logs, which shows a salt-water-to-highly-brackish water plume contaminating the alluvial aquifer: **a** salt-water-to-highly-brackish water plume contaminating a sandy body within the alluvial aquifer and shallow low-resistivity anomalies within the upper clayey deposits; **b** slightly brackish-to-freshwater contaminating clayey sandy deposits. The resistivity model shows good correlation with respect to well 30 logs which found a drop in resistivity at 11 m depth, along with an increase of temperature and a decrease of redox potential of groundwater, suggesting a well transition zone between slightly brackish to moderate brackish water

bedrock depth. Geophysical results enabled detailed localization and tracing of the Vogherese Fault at the scale of the investigated area. Other minor subparallel structural discontinuities (faults and fractures) were also identified. These minor discontinuities show geometries and directions (NW–SW) that are coherent with those of the Vogherese Fault and are therefore genetically connected to the major structural discontinuity.

The bedrock is affected by the presence of Na–Cl paleowaters which are likely localized along structural discontinuities which represent preferential flow paths for the saline waters and facilitate the flow towards the alluvial aquifer. The contamination is strictly controlled by the geological and structural configuration of the area. The morphology of the tertiary bedrock and the spatial distribution of the structural discontinuities are likely to be partially controlling the distribution of salty groundwater, originating at depth, within the alluvial aquifer.

The spatial distribution of Na–Cl waters suggests the existence of plumes of highly mineralized waters that locally reach the aquifer, diffuse and mix with freshwaters. Detailed 3D imaging revealed irregular-shaped shallow saline-water contamination areas within the alluvial aquifer.

Overall, the salt-water-saturated clayey bedrock shows resistivity values lower than 3 Ω·m, while salt-water-saturated sandy alluvial deposits show resistivity values ranging between 3 and 8 Ω·m; brackish-water saturated sandy alluvial deposits show resistivity values ranging between 8 and 12 Ω·m; slightly brackish waters to freshwaters are associated with bulk resistivity values ranging between 30 and 78 Ω·m. The interpretation of these resistivity ranges is consistent with findings from Torrese and Pilla (2021) who calibrated resistivity surveys with well logs in the same area investigated in this study. Even if these ranges of values can be considered representative for such a geological setting, it is worth underlining that the resistivity of such hydrogeological bodies does not depend on the electrical conductivity of the fluid only, but also on the porosity and clay content of the solid material. Moreover, the resistivity signature depends even on the size of the body in relation to its depth and on the contrast between the resistivity of the body and that of the surrounding rock. This is the reason why the same hydrogeological body can show slightly different resistivity values even in the same site.

Contamination from saline waters is not spatially and vertically homogeneous within the aquifer. This

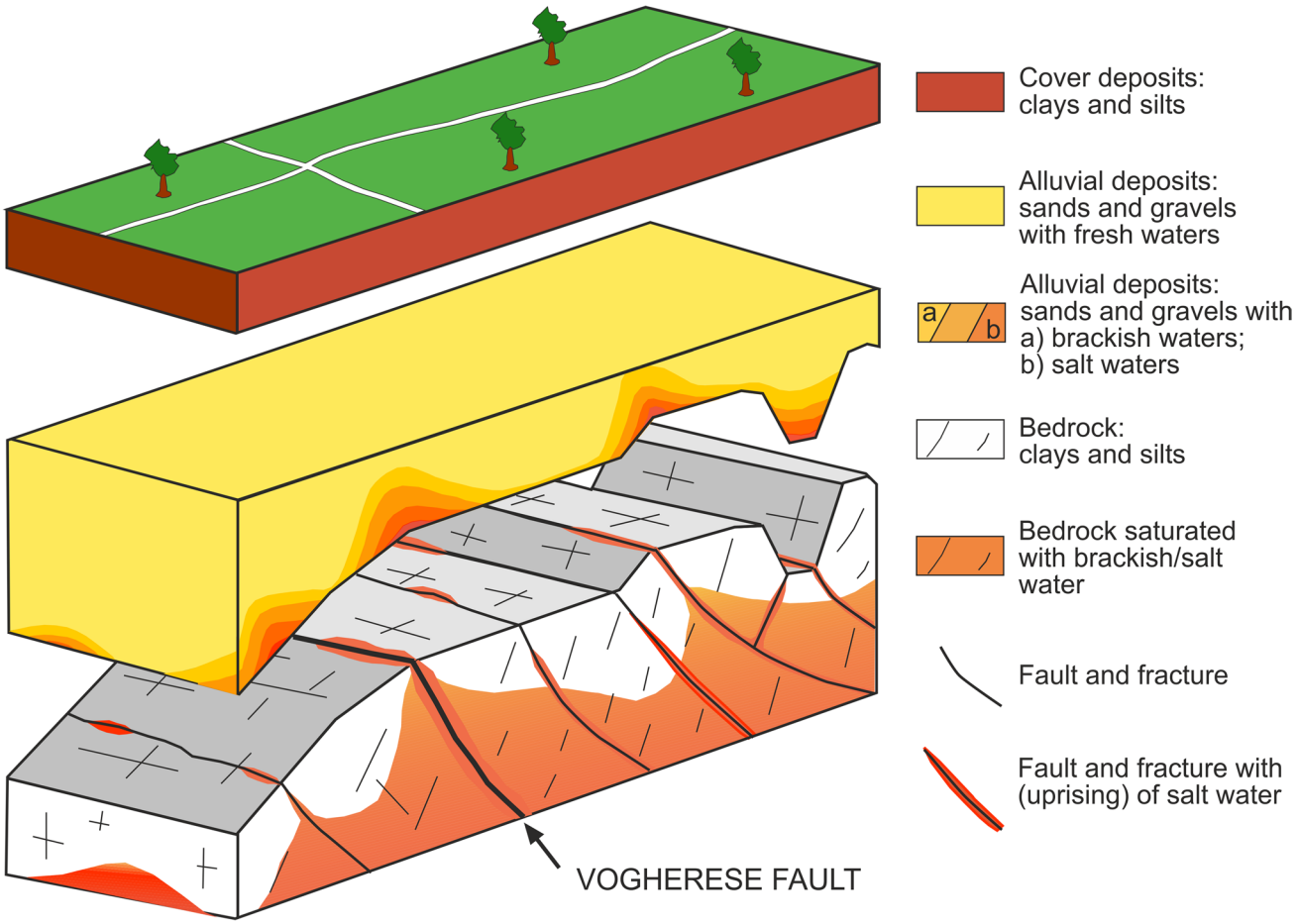

Fig. 13 Small-scale simplified hydrogeological conceptual model of the investigated area as revealed by hydrochemical and geophysical investigations. Figure modified from Torrese and Pilla (2021)

nonhomogeneity is likely to be affected by different factors like the aperture of the discontinuities within the hydrogeological bedrock, and the hydraulic conductivity of the aquifer, as well as seasonal variations in terms of freshwater recharge and groundwater pumping. The observed variability of salinity and depth of the transition zone can be attributed to the distance of the monitored wells from the center of the plume.

Salt water intrusion into the alluvial aquifer has a heterogeneous distribution, and suggests the existence of plumes of highly mineralized waters that locally reach the aquifer, diffuse and mix with freshwaters. Deep saline paleo-waters show a dilution during upward migration. The hydrodynamic flow of shallow fresh groundwater would tend to relegate the highly mineralized groundwater to the lower sections of the aquifer.

This interpretation can explain the different degrees of groundwater salinity detected in the course of the investigations and also the different characteristics of the transition zone into the same area. In fact, wells located on a plume show higher values of water electrical conductivity and a shallower depth of the freshwater/salt-water interface. The distribution of the plumes is influenced mostly by the presence of tectonic discontinuities into the marine substratum but, probably, also by the local hydraulic permeability of the alluvial sediments. There is a lower degree of contamination in those sectors of the aquifer that are further away from the structural discontinuities and this lower degree of contamination generally only involves the deeper parts of the aquifer.

The overall simplified hydrogeological conceptual model of the investigated area is shown in Fig. 13. This model represents the main features of the shallow aquifer as revealed by hydrochemical and geophysical investigations. It shows the plumes of high-salinity groundwater that reach the alluvial aquifer. Here, they diffuse and mix with the fresh groundwater of the shallow aquifer, thus originating different degrees of groundwater salinity within the aquifer. Highly mineralized groundwater is identified even at very shallow depth in correspondence of each plume, which is located above a structural discontinuity.

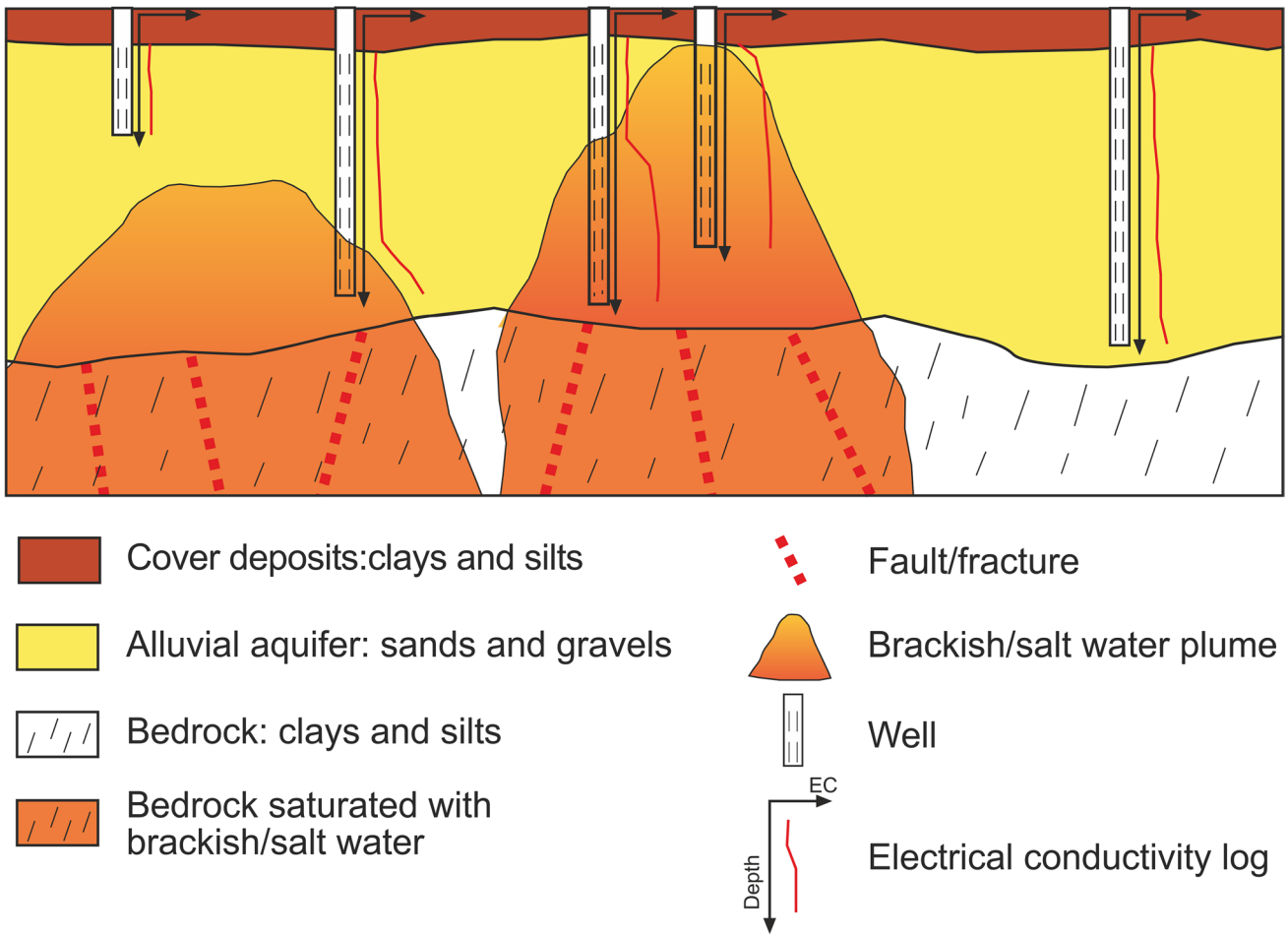

Fig. 14 Large-scale simplified hydrogeological conceptual model of the investigated area which shows the presence of salt-water plumes that reach the alluvial aquifer, as revealed by hydrochemical and geophysical investigations

A detailed simplified hydrogeological conceptual model of the investigated area is shown in Fig. 14. This model shows that the contamination from saline waters is not spatially and vertically homogeneous even at the scale of the well field. The wells located on a plume show higher values of water electrical conductivity and a shallower depth of the freshwater/salt-water interface. Moreover, the hydrodynamic flow of shallow fresh groundwater would tend to relegate the highly mineralized groundwater to the lower sections of the aquifer. However, it cannot categorically be ruled out that in the deeper portions of the alluvial aquifer, the development of the saline plumes is also conditioned by differences in hydraulic head between the deep brine reservoir and the shallow alluvial aquifer and by local variations in hydraulic conductivity within the alluvial deposits.

The study shows that it is necessary to use a multidisciplinary approach (which includes the integration of hydrochemical and geophysical investigations within the hydrogeological assessment), when it comes to understanding extremely complex forms of groundwater natural contamination, similar to the contamination that has been identified in the Oltrepò Pavese area, where several intervening factors can influence the contamination.

Future studies may be based on the correlation between the temporal variability of groundwater salinity and the variability in the discharge of uprising salt water. These studies would allow one to verify if the uprise of salt water is likely to be induced by an increase in hydraulic head within the main Apennine groundwater following rainfall or snow melting events. This system could be in hydraulic connection with a deeper aquifer that host saline waters. The pressure transfer, through a piston flow mechanism (Pilla et al. 2010; Re and Zuppi 2011), may produce a mass transfer where saline waters are forced to rise along discontinuities and reach the shallow aquifer. Forthcoming studies based on continuous piezometric and hydrochemical monitoring of the alluvial aquifer groundwater correlated to rainfall or snow melting events in the nearby Apennines will allow one to verify the piston-flow-mechanism-based hypothesis.

Conclusions

This paper presents an integrated hydrochemical and geophysical study of saline paleo-water uprising into the alluvial aquifer of the Oltrepò Pavese plain sector (Po Plain, northern Italy). This study involved periodical sampling of groundwater, vertical electrical conductivity and temperature logs, and geophysical surveys. These involved both EM surveys undertaken over vast areas for a speedy assessment of subvertical conductive bodies connected to the uprising of high-salinity waters through structural discontinuities and more accurate 1D–3D electric resistivity surveys for detailed investigation of the sectors where the uprising phenomena of deep saline waters occurs.

In this area, the alluvial aquifer is strongly conditioned by the presence of the Vogherese Fault, a buried tectonic discontinuity along which the saline waters are mainly distributed. These Na–Cl-rich waters rise along the discontinuities in the hydrogeological bedrock and flow into the overlying alluvial aquifer. This particular setting conditions the distribution of saline waters into the alluvial aquifer.

Contamination from saline waters is not spatially and vertically homogeneous within the aquifer. The spatial distribution of Na–Cl waters suggests the existence of plumes of highly mineralized waters that locally reach the aquifer, diffuse and mix with freshwaters. Detailed 3D imaging revealed irregular-shaped shallow saline-water contamination within the alluvial aquifer.

Deep saline paleo-waters show a dilution during upward migration, which is due to the mixing with shallow fresh groundwater. Highly mineralized groundwater is identified even at very shallow depth in correspondence of each plume, and is located above a structural discontinuity. On the other hand, there is a lower degree of contamination in those sectors of the aquifer that are further away from the structural discontinuities and generally only involves the deeper parts of the aquifer.

Forthcoming studies, based on continuous piezometric and hydrochemical monitoring of the alluvial aquifer groundwater correlated to rainfall or snow melting events in the nearby Apennine mountain range, will allow one to verify if the uprise of salt water is to be induced by an increase in hydraulic head within the main Apennine groundwater. The pressure transfer, through a piston flow mechanism, could produce a mass transfer where saline waters are forced to rise along discontinuities and reach the shallow aquifer.

The results from this study are applicable in similar hydrogeological contexts where the aquifer's contamination by saline water is caused by mixing of freshwaters with brines or where the fossil salt water, located several kilometers from the coastline, are the remainder of ancient marine ingressions.

Supplementary Information The online version contains supplementary material available at https://doi.org/10.1007/s10040-021-02446-5.

Acknowledgements The study was developed in the framework of the convention between Dipartimento di Scienze della Terra e dell'Ambiente of Università di Pavia (P.I. Giorgio Pilla) and Provincia di Pavia - Settore Tutela Ambientale with the collaboration of Comune di Casteggio, Comune di Santa Giuletta, Comune di Montebello della Battaglia, the company Pavia Acque Srl and the company Casteggio Lieviti Srl. The authors are grateful to Marica Bersan, Massimiliano Bordoni, Luca Bovolenta, Alessandro Sartirana and Francesco Tosi for their support in data collection, processing and editing. We would like to thank the people that allowed us to access and sample the investigated area. The authors wish to thank the editor Jean-Michel Lemieux, associate editor Kevin Befus and two anonymous reviewers who kindly reviewed an earlier version of the manuscript and provided valuable suggestions and comments, greatly improving the quality of the paper.

Declarations

Conflict of interest The authors declare that they have no known competing financial interests or personal relationships that could have appeared to influence the work reported in this paper.

References

AGIP (1972) Acque dolci sotterranee [Fresh underground waters]. AGIP S.p.A. Direzione Generale Servizi Centrali per l'Esplorazione, Grafica Palombi, Rome, 914 pp

Adepelumi AA, Yi MJ, Kim JH, Ako BD, Son J-S (2006) Integration of surface geophysical methods for fracture detection in crystalline bedrocks of southwestern Nigeria. Hydrogeol J 14:1284–1306. https://doi.org/10.1007/s10040-006-0051-2

Akouvi A, Dray M, Violette S, De Marsily G, Zuppi GM (2008) The sedimentary coastal basin of Togo: example of a multilayered aquifer still influenced by a palaeo-seawater intrusion. Hydrogeol J 16:419–436

Al-Tarazi E, Abu Rajab J, Al-Naqa A, El-Waheidi M (2008) Detecting leachate plumes and groundwater pollution at Ruseifa municipal landfill utilizing VLF-EM method. J Appl Geophys 65:121–131

Appelo CAJ, Postma D (2005) Geochemistry, groundwater and pollution, 2nd edn. Balkema, Rotterdam, 683 pp

Arato A, Godio A, Sambuelli L (2014) Staggered grid inversion of cross hole 2-D resistivity tomography. J Appl Geophys 107:60–70

Athanasiou EN, Tsourlos PI, Papazachos CB, Tsokas GN (2007) Combined weighted inversion of electrical resistivity data arising from different array types. J Appl Geophys 62(2):124–140

Barberio MD, Gori F, Barbieri M, Boschetti T, Caracausi A, Cardello GL, Petitta M (2021) Understanding the origin and mixing of deep fluids in shallow aquifers and possible implications for crustal deformation studies: San Vittorino plain, Central Apennines. Appl Sci 11:1353. https://doi.org/10.3390/app11041353

Bersan M, Bocca B, Ciancetti G, Dolza G, Meisina C, Pilla G (2007) Deep chemical anomalous groundwaters of the Pavia-Piacenza Apennine and its foreland (Po Plain). Geoitalia 2007, Rimini, Italy, 12–15September 2007, 180 pp

Bersan M, Pilla G, Dolza G, Torrese P, Ciancetti G (2010) The uprising of deep saline waters into the Oltrepò Pavese (northern Italy) aquifer: early results. Ital J Eng Geol Environ 1:7–22

Boni A (1967) Note illustrative della Carta Geologica d'Italia [Explanatory notes of the geological map of Italy]. F. 59 Pavia, Servizio Geologico d'Italia, Rome, 68 pp

Bonnesen EP, Larsen F, Sonnenborg TO, Klitten K, Stemmerik L (2009) Deep saltwater in Chalk of North-West Europe: origin, interface characteristics and development over geological time. Hydrogeol J 17:1643–1663. https://doi.org/10.1007/s10040-009-0456-9

Bonori O, Ciabatti M, Cremonini S, Di Giovambattista R, Martinelli G, Maurizi S, Quadri G, Rabbi E, Righi PV, Tinti S, Zantedeschi E (2000) Geochemical and geophysical monitoring in tectonically active areas of the Po Valley (northern Italy): case histories linked to gas emission structures. Geog Fis Din Quater 23:3–20

Boschetti T, Toscani L, Shouakar-Stash O, Iacumin P, Venturelli G, Mucchino C, Frape SK (2011) Salt waters of the northern Apennine Foredeep Basin (Italy): origin and evolution. Aquat Geochem 17(1):71–108. https://doi.org/10.1007/s10498-010-9107-y

Bouchaou L, Michelot JL, Mohamed Q, Zine N, Gaye CB, Aggarwal P, Marah H, Zerouali A, Taleb H, Vengosh A (2009) Origin and residence time of groundwater in the Tadla Basin (Morocco) using multiple isotopic and geochemical tools. J Hydrol 379:323–338. https://doi.org/10.1016/j.jhydrol.2009.10.019

Bowling JC, Rodriguez AB, Harry DL, Zheng C (2005) Delineating alluvial aquifer heterogeneity using resistivity and GPR data. Groundwater 43(6):890–903. https://doi.org/10.1111/j.1745-6584.2005.00103.x

Braga G, Cerro A (1988) Le strutture sepolte della pianura pavese e le relative influenze sulle risorse idriche sotterranee [The buried structures of the Pavia plain and the related influences on underground water resources]. Atti Tic Sci Terra 31:421–433

Buvat S, Schamper C, Tabbagh A (2013) Approximate three-dimensional resistivity modelling using Fourier analysis of layer resistivity in shallow soil studies. Geophys J Int 194(1):158–169

Cameron E, Pilla G, Stella FA (2018) Application of statistical classification methods for predicting the acceptability of well-water quality. Hydrogeol J 26:1099–1115

Cassiani G, Godio A, Stocco S, Villa A, Deiana R, Frattini P, Rossi M (2009) Monitoring the hydrologic behaviour of a mountain slope via time-lapse electrical resistivity tomography. Near Surface Geophys 7:475–486

Cavanna F, Marchetti G, Vercesi PL (1998) Idrogeomorfologia e insediamenti a rischio ambientale: il caso della pianura dell'Oltrepò Pavese e del relativo margine collinare [Hydrogeomorphology and environmental risk settlements: the case of the Oltrepò Pavese plain and its hilly margin]. Fondazione Lombardia Ambiente, Isabel Litografia, Gessate, Italy

Conti A, Sacchi E, Chiarle M, Martinelli G, Zuppi GM (2000) Geochemistry of the formation water of the Po plain (northern Italy): an overview. Appl Geochem 15:51–65

Coscia I, Greenhalgh SA, Linde N, Doetsch J, Marescot L, Günther T, Vogt T, Green AG (2011) 3D crosshole ERT for aquifer characterization and monitoring of infiltrating river water. Geophysics 76(2):G49. https://doi.org/10.1190/1.3553003

Cotecchia V, Limoni PP, Polemio M (1999) Identification of typical chemical and physical conditions in Apulian groundwater (southern Italy) through well multi-parameter logs. 39th IAH Congress, Bratislava, Slovakia, pp 353–358

Dahlin T, Loke MH (1998) Resolution of 2-D Wenner resistivity imaging as assessed by numerical modelling. J Appl Geophys 38:237–249

Daily W, Owen E (1991) Crosshole resistivity tomography. Geophysics 56:1228–1235

Daily W, Ramirez A (1992) Electrical resistivity tomography of vadose water movement. Water Resour Res 28:1429–1442

Darling WG, Edmunds WM, Smedley PL (1997) Isotopic evidence for palaeowaters in the British Isles. Appl Geochem 12(6):813–829. https://doi.org/10.1016/S0883-2927(97)00038-3

Desiderio G, Rusi S (2004) Idrogeologia e idrogeochimica delle acque mineralizzate dell'Avanfossa Abruz zese Molisana [Hydrogeology and hydrogeochemistry of the mineralized waters of the Avanfossa Abruz zese Molisana]. Boll Soc Geol Ital 123:373–389

Dever L, Travi Y, Barbecot F, Marlin C, Gibert E (2001) Evidence for palaeowaters in the coastal aquifers of France. Geol Soc Lond Spec Publ 189:93–106. https://doi.org/10.1144/GSL.SP.2001.189.01.07

Di Sipio E, Galgaro A, Zuppi GM (2006) New geophysical knowledge of groundwater system in Venice estuarine environment. Estuarine Coastal Shelf Sci 66:6–12

Di Sipio E, Galgaro A, Zuppi GM (2007) Contaminazione salina nei sistemi acquiferi dell'entroterra me ridionale della laguna di Venezia [Saline contamination in the aquifer systems of the southern hinterland of the Venice lagoon]. G Geol Appl 5:5–12

Fadili A, Najib S, Mehdi K, Riss J, Malaurent P, Makan A (2017) Geoelectrical and hydrochemical study for the assessment of seawater intrusion evolution in coastal aquifers of Oualidia, Morocco. J Appl Geophys 146:178–187

Gómez E, Larsson M, Dahlin GT, Barmen G, Rosberg JE (2019) Alluvial aquifer thickness and bedrock structure delineation by electromagnetic methods in the highlands of Bolivia. Environ Earth Sci 78:84. https://doi.org/10.1007/s12665-019-8074-x

Gnaneshwar P, Shivaji A, Srinivas Y, Jettaiah P, Sundararajan N (2011) Very-low-frequency electromagnetic (VLF-EM) measurements in the Schirmacheroasen area, East Antarctica. Polar Sci. https://doi.org/10.1016/j.polar.2010.09.001

Griffiths DH, Barker RD (1993) Two-dimensional resistivity imaging and modeling in areas of complex geology. J Appl Geophys 29:211–226

Grobe M, Machel HG (2002) Saline groundwater in the Münsterland cretaceous basin, Germany: clues to its origin and evolution. Mar Pet Geol 19:307–322

Guérin R, Benderitter Y (1995) Shallow karst network exploration using MT-VLF and DC resistivity methods. Geophys Prospect 43(5):635–653

Guérin R, Bégassat P, Benderitter Y, David J, Tabbagh A, Thiry M (2004) Geophysical study of the industrial waste land in Mortagne-du-Nord (France) using electrical resistivity. Near Surface Geophys 2(3):137–143

Hinsby K, Harrar WG, Nyegaard P, Konradi PB, Rasmussen ES, Bidstrup T, Gregersen U, Boaretto R (2001) The Ribe formation in western Denmark: Holocene and Pleistocene groundwaters in a coastal Miocene sand aquifer. In: Palaeowaters in coastal Europe: evolution of groundwater since the late Pleistocene. Geol Soc Spec Publ 189

Italian Legislature (2001) Decreto Legislativo 2 febbraio (2001) n. 31 - Attuazione della direttiva 98/83/CE relativa alla qualità delle acque destinate al consumo umano [Legislative Decree 2 February (2001) no. 31: implementation of Directive 98/83 / EC relating to the quality of water intended for human consumption]. Gazzetta

Ufficiale n. 52 del 3 marzo 2001 - Supplemento Ordinario n. 41, Italian Legislature, Rome
Jamal N, Singh NP (2018) Identification of fracture zones for groundwater exploration using very low frequency electromagnetic (VLF-EM) and electrical resistivity (ER) methods in hard rock area of Sangod Block, Kota District, Rajasthan, India. Groundw Sustain Dev 7:195–203, ISSN 2352-801X. https://doi.org/10.1016/j.gsd.2018.05.003
Jiraporn S-J, Srilert C, Thanop T (2020) Hydrochemical, geophysical and multivariate statistical investigation of the seawater intrusion in the coastal aquifer at Phetchaburi Province, Thailand. J Asian Earth Sci 191:104165. https://doi.org/10.1016/j.jseaes.2019.104165
Kazakis N, Pavlou A, Vargemezis G, Voudouris KS, Soulios G, Pliakas F, Tsokas G (2016) Seawater intrusion mapping using electrical resistivity tomography and hydrochemical data: an application in the coastal area of eastern Thermaikos Gulf, Greece. Sci Total Environ 543:373–387. https://doi.org/10.1016/J.SCITOTENV.2015.11.041
Kneisel C (2006) Assessment of subsurface lithology in mountain environments using 2D resistivity imaging. Geomorphology 80(1–2):32–44. https://doi.org/10.1016/j.geomorph.2005.09.012
Kouzana L, Benassi R, Ben Mammou A, Felfoul M (2010) Geophysical and hydrochemical study of the seawater intrusion in Mediterranean semi arid zones: case of the Korba coastal aquifer (Cap-Bon, Tunisia). J Afr Earth Sci 58:242–254
Kuras O, Pritchard JD, Meldrum PI, Chambers JE, Wilkinson PB, Ogilvy RD, Wealthall GP (2009) Monitoring hydraulic processes with automated time-lapse electrical resistivity tomography (ALERT). C R Geosci - Spec Issue Hydrogeophys 341:868–885
LaBrecque DJ, Miletto M, Daily W, Ramirez A, Owen E (1996) The effects of noise on Occam's inversion of resistivity tomography data. Geophysics 61:538–548
Loke MH, Acworth I, Dahlin T (2003) A comparison of smooth and blocky inversion methods in 2-D electrical imaging surveys. Explor Geophys 34:182–187
Loke MH, Barker RD (1996) Rapid least-squares inversion of apparent resistivity pseudosections by a quasi-Newton method. Geophys Prospect 44(1):131–152. https://doi.org/10.1111/j.1365-2478.1996.tb00142.x
Marandi A, Vallner L (2010) Upconing of saline water from the crystalline basement into the Cambrian-Vendian aquifer system on the Kopli Peninsula, northern Estonia. Estonian J Earth Sci 59:277–287. https://doi.org/10.3176/earth.2010.4.04
Meyerhoff SB, Karaoulis M, Fiebig F, Maxwell RM, Revil A, Martin JB, Graham WD (2012) Visualization of conduit-matrix conductivity differences in a karst aquifer using time-lapse electrical resistivity. Geophys Res Lett 39:L24401. https://doi.org/10.1029/2012GL053933
Meyerhoff SB, Maxwell RM, Revil A, Martin JB, Karaoulis M, Graham WD (2014) Characterization of groundwater and surface water mixing in a semiconfined karst aquifer using time-lapse electrical resistivity tomography. Water Resour Res 50:2566–2585. https://doi.org/10.1002/2013WR013991
Morelli G, LaBrecque DJ (1996) Advances in ERT inverse modelling. Eur J Environ Eng Geophys Soc 1(2):171–186
Nanni T, Zuppi GM (1986) Acque salate e circolazione profonda in relazione all'assetto strutturale del fronte adriatico e padano dell'Appennino [Salt water and deep circulation in relation to the structural set-up of the Adriatic and Po Valley of the Apennines]. Mem Soc Geol It 35:979–986
Ohwoghere-Asuma O, Chinyem IF, Aweto KE, Iserhien-Emekeme R (2020) The use of very low-frequency electromagnetic survey in the mapping of groundwater condition in Oporoza-Gbamaratu area of the Niger Delta. Appl Water Sci 10:164. https://doi.org/10.1007/s13201-020-01244-w
Paal G (1965) Ore prospecting based on VLF radio signals. Geoexploration 3:139–147
Parker ME (1980) VLF electromagnetic mapping for strata-bound mineralization near Aberfeldy, Scotland. Trans Inst Min Metall Sect B 89:B123–B133
Paterson NR, Ronka V (1971) Five years of surveying with the very low frequency electromagnetic method. Geoexploration 9:7–26
Pellegrini L, Vercesi PL (1995) Considerazioni morfotettoniche sulla zona a sud del Po tra Voghera (PV) e Sarmato (PC) [Morphotectonic considerations on the area south of the Po between Voghera (PV) and Sarmato (PC)]. Atti Tic Sci Terra 38:95–118
Petitta M, Primavera P, Tuccimei P, Aravena R (2011) Interaction between deep and shallow groundwater systems in areas affected by Quaternary tectonics (central Italy): a geochemical and isotope approach. Environ Earth Sci 63:11–30
Phillips WJ, Richards WE (1975) A study of the effectiveness of the VLF method for the location of narrow mineralized zones. Geoexploration 13:215–226
Pilla G, Sacchi E, Ciancetti G (2007) Hydrogeologic, hydrochemical and isotopic groundwater investigation in the plain of the Oltrepò Pavese region (southern Lombardy, Italy). G Geol Appl 5:59–74
Pilla G, Torrese P, Bersan M (2010) Application of hydrochemical and preliminary geophysical surveys within the study of the saltwater uprising occurring in the Oltrepò Pavese plain aquifer. Boll Geofis Teor Appl 51(4):301–323
Polemio M, Dragone V, Limoni PP (2009) Monitoring and methods to analyse the groundwater quality degradation risk in coastal karstic aquifers (Apulia, southern Italy). Environ Geol 58(2):299–312
Pujari PR, Padmakar C, SuriNaidu L et al (2012) 2012. Integrated hydrochemical and geophysical studies for assessment of groundwater pollution in basaltic settings in central India. Environ Monit Assess 184:2921–2937. https://doi.org/10.1007/s10661-011-2160-1
Rainone ML, Rusi S, Torrese P (2015) Mud volcanoes in central Italy: subsoil characterization through a multidisciplinary approach. Geomorphology 234:228–242. https://doi.org/10.1016/j.geomorph.2015.01.026
Ramesh Babu V, Ram S, Sundararajan N (2007) Modeling of magnetic and VLF-EM with an application to basement fractures: a case study from Raigad, India. Geophysics 71:133e140
Re V, Zuppi GM (2011) Influence of precipitation and deep saline groundwater on the hydrological systems of Mediterranean coastal plains: a general overview. Hydrol Sci J 56(6):966–980
Regione Lombardia and ENI Divisione AGIP (2002) Geologia degli acquiferi padani della Regione Lombardia: relazione tecnica [Geology of the Po aquifers of the Lombardy Region: technical report]. S.EL.CA., Florence
Ritz M, Robain H, Pervago E, Albouy Y, Camerlynck C, Descloitres M, Mariko A (1999) Improvement to resistivity pseudosection modelling by removal of near-surface heterogeneity effects: application to a soil system in South Cameroon. Geophys Prospect 47:85–101
Saydam AS (1981) Very low frequency electromagnetic interpretation using tilt angle and ellipticity measurements. Geophysics 46:1594–1606
Schrott L, Sass O (2008) Application of field geophysics in geomorphology: advances and limitations exemplified by case studies. Geomorphology 93(1–2):55–73. https://doi.org/10.1016/j.geomorph.2006.12.024
Schwartz FW, Muehlenbachs K (1979) Isotope and ion geochemistry of groundwaters in the Milk River aquifer, Alberta. Water Resour Res 15:259–268

Shin J, Hwang S (2020) A borehole-based approach for seawater intrusion in heterogeneous coastal aquifers, eastern part of Jeju Island, Korea. Water 12:609. https://doi.org/10.3390/w12020609

Smart CC, Worthington SRH (2003) Electrical conductivity profiling of boreholes as a means of identifying karst aquifers. Geotech Spec. Publ. no. 122, Am. Soc. Civil Engineers, Reston, VA, pp 265–276

Smith DL (1986) Application of the pole–dipole resistivity technique to the detection of solution cavities beneath highways. Geophysics 51(3):833–837

Spiegel RJ, Sturdivant VR, Owen TE (1980) Modeling resistivity anomalies from localized voids under irregular terrain. Geophysics 45:1164–1183

Sundararajan N, Ramesh Babu V, Shiva Prasad N, Srinivas Y (2006) VLFPROSda MATLAB code for processing of VLF-EM data. Comput Geosci 32:1806e1813

Szalai S, Szarka L (2008) Parameter sensitivity maps of surface geoelectric arrays: I. linear arrays. Acta Geodaet Geophys Hungarica 43(4):419–437. https://doi.org/10.1556/AGeod.43.2008.4.4

Szalai S, Novak A, Szarka L (2009) Depth of investigation and vertical resolution of surface geoelectric arrays. J Environ Eng Geophys 14(1):15–23. https://doi.org/10.2113/JEEG14.1.15

Stueber AM, Saller A, Ishida H (1998) Origin, migration, and mixing of brines in the Permian Basin: geo chemical evidence from the eastern Central Basin Platform, Texas. AAPG Bull 82:1652–1672

Tal A, Weinstein Y, Baïsset M, Golan A, Yechieli Y (2019) High-resolution monitoring of seawater intrusion in a multi-aquifer system: implementation of a new downhole geophysical tool. Water 11(9):1877

Torrese P (2020) Investigating karst aquifers: using pseudo 3-D electrical resistivity tomography to identify major karst features. J Hydrol 580, 124257. https://doi.org/10.1016/j.jhydrol.2019.124257

Torrese P, Pilla G (2021) 1D–4D electrical and electromagnetic methods revealing fault-controlled aquifer geometry and saline water uprising. J Hydrol 126568. https://doi.org/10.1016/j.jhydrol.2021.126568

Torrese P, Pozzobon R, Rossi AP, Unnithan V, Sauro F, Borrmann D, Lauterbach H, Santagata T (2021) Detection, imaging and analysis of lava tubes for planetary analogue studies using electric methods (ERT). Icarus 357. https://doi.org/10.1016/j.icarus.2020.114244

Toscani L, Boschetti T, Maffini M, Barbieri M, Mucchino C (2007) The groundwaters of Fontevivo (Parma Province, Italy): redox processes and mixing with brine waters. Geochem Explor Environ Analysis 7:2

Vandenbohede A, Mollema PN, Greggio N, Antonellini M (2014) Seasonal dynamic of a shallow freshwater lens due to irrigation in the coastal plain of Ravenna, Italy. Hydrogeol J 22:893–909

Van Schoor M (2002) Detection of sinkholes using 2D electrical resistivity imaging. J Appl Geophys 50(4):393–399. https://doi.org/10.1016/S0926-9851(02)00166-0

Vogelgesang JA, Holt N, Schilling KE, Gannon M, Tassier-Surine S (2020) Using high-resolution electrical resistivity to estimate hydraulic conductivity and improve characterization of alluvial aquifers. J Hydrol 580:123992. https://doi.org/10.1016/j.jhydrol.2019.123992

Wilcox LV (1948) The quality of water for irrigation use. USDA Tech Bull 962:1–40

Yechieli Y, Sivan O (2010) The distribution of saline groundwater and its relation to the hydraulic conditions of aquifers and aquitards: examples from Israel. Hydrogeol J 19:71–81